

# Optics calculation for the Hall D tagging spectrometer magnet for a 12 GeV electron beam

Guangliang Yang

Department of Physics and Astronomy,  
Glasgow University, Glasgow, G12 8QQ

By using the computer code TRANSPORT, the tagging spectrometer magnet optical properties have been calculated. The parameters investigated are the tilt angle and the radius of curvature of the output edge, the width of the magnet pole shoe, the object distance, the beam entrance angle, and having a quadrupole before the dipole. Their effects on the resolution, dispersion, beam vertical spot size and other properties have been systematically studied. It was found, by decreasing the tilt angle and/or increasing the width of the magnet pole shoe and/or increasing the object distance, the electron resolution can be dramatically reduced. But, at the same time, in order to obtain a short and simply shaped focal plane, we should use a relatively larger tilt angle; and in order to obtain a larger momentum acceptance, we should use smaller width of the magnet pole shoe; in order to avoid the beam vertical size exceeding the magnet gap, the object distance should be not too large. A curved output edge gives a shorter focal plane and requires less vacuum volume, but the resolution is a little worse than for the straight output edge case. By using a quadrupole configuration, the beam vertical height can be dramatically reduced, and the resolution also is slightly improved. In the studied range, the entrance angle has little effect on the focal plane, and a larger entrance angle gives slightly better resolution. By considering the effects of all the parameters, suitable parameters for the magnet have been selected.

## 1. Introduction

The CEBAF upgrade to the energy of 12 GeV gives an opportunity to generate high-energy polarized bremsstrahlung photons at around 9 GeV for high-energy photo-production experiments. An important part of this upgrade is to build a high performance spectrometer to measure the photon energies. The spectrometer is composed of a room temperature electromagnet and some other elements. The magnet is the most important part of the spectrometer, which determines the optical properties of the spectrometer. But, for a room temperature magnet, it is difficult to obtain a uniformly distributed magnetic field of more than 2 T. Due to this relatively low magnetic field and the large electron momentum, the radius of curvature for the main beam is very large. For example, for a 1.5T magnetic field, the radius of curvature for a 12 GeV electron beam is 26.685m, so if we use a standard Elbek type magnet, the magnet size will be very large. In order to obtain a reasonable magnet size, the main beam bend angle is reduced to 13.4 degrees[1]. The reduction in the bend angle affects the performance of the spectrometer, and other spectrometer parameters such as the tilt angle and the radius of curvature of the magnet output edge, the incident beam rotation angle, the object distance etc also have significant effects on the spectrometer performance. To obtain the best performance of the spectrometer, we need to know the effects of these parameters on the spectrometer properties. In the present report, by using the computer code TRANSPORT, these effects have been studied.

A plan view of the spectrometer magnet is shown in Fig. 1. The line segment AIB is the input edge, the line segment BCD is the output edge, the line segment DEF is the main beam exit edge and the line segment FGA is the back edge. A radiator is located at the point O, and the distance from O to I is the object distance. The tilt angle of the output edge is the angle between the output edge and the line segment DEF. The line segment DEF is perpendicular to the main beam. The bend angle of the main beam is fixed at 13.4 degrees. In designing the magnet geometry, three parameters can be changed, i.e. the tilt angle and the radius of curvature of the output edge, and the length of the line segment DE.

The main beam properties are listed in table 1. As input data for the computer code TRANSPORT, the scattered electrons (see table 2) were assumed to have the same size as the main beam but with a maximum beam divergence given by the formula estimated from the practical angular divergence of bremsstrahlung electrons [2].

$$\Delta y' = \frac{4mc}{E_0} \times \frac{E_0 - E}{E}$$

Where,  $E_0$  and  $E$  are the beam energy and the scattered electron energy respectively,  $m$  is the mass of electron, and  $c$  is the velocity of photon in the vacuum. Here, we assume the electron beam follows a Gaussian distribution. The object size is assumed to be equal to  $4\Delta x$  ( $\Delta x$  is the square root of the variance of the beam radial distribution). This represents the worst case for the spectrometer

since, in reality, the scattered electrons are not evenly distributed, with about 68 % being located within the central  $2\Delta x$  region. The field profile in the dipole is assumed to be constant within the central area with a fringe field on both input and output edges. The electron resolution is defined as[3]

$$R = \frac{\Delta\omega}{D}$$

where  $\Delta\omega$  is half the radial image size in the focal plane and  $D$  is the dispersion, both of which are calculated by TRANSPORT.

## 2. The effects of the tilt angle and the radius of curvature of the output edge.

In this section, we focus on the effects of varying the tilt angle and the radius of curvature of the output edge on the spectrometer properties. The studied radii of curvature are 30m, 50m, 100m, and finally infinity (The output edge becomes straight). The tilt angles decrease from the initial angle selected with a step of 0.2 degree, 0.4 degree, 0.5 degree and 0.5 degree respectively for the 4 radii selected. The initial angle is the tilt angle when the output edge approximately goes through the point where the incident beam intercepts with the input edge. The object distance is 2m, and the incident beam entrance angle is 0 degree. The studied electron energy range is 10-75% $E_0$ .

Fig. 2 shows the focal plane position (shown by the blue triangles) corresponding to the different geometrical structures of the magnet with different tilt angles and different radii of curvature of the output edge. In Fig 2.1, the tilt angle changes from 83.5 to 80.5 degrees with a step of  $-0.5$  degrees, and the output edge is straight. It is found that it has a nearly straight focal plane when the tilt angle is not too far from the initial angle. By decreasing the tilt angle, the focal plane becomes slightly curved, and the length of the focal plane and the distance from the focal plane to the output edge increase. The upper part of the focal plane is further from the output edge than the lower part of the focal plane. In Fig 2.2, the tilt angle changes from 85 to 82.5 degrees with a step of  $-0.5$  degrees, and the output edge is curved, with a radius of curvature of 100m. In this case, the focal plane position changes with a similar trend to the straight output edge case. But the distance from the focal plane to the output edge in the middle of the focal plane is slightly smaller than that for the straight output edge case. In Fig 2.3, the tilt angle changes from 86.8 to 84.8 degrees with a step of  $-0.4$  degrees, and the output edge is curved, with a radius of curvature of 50m. The trend is similar to the first two cases. The distance from the focal plane to the output edge in the middle of the focal plane is obviously smaller than that for the straight output edge case. We are very interested in the situation shown by fig2.3b. In this situation, the focal plane is nearly parallel to the output edge, which is beneficial for designing a smaller vacuum space. In Fig 2.4, the tilt angle changes from 89.2 to 88.2 degrees with a step of  $-0.2$  degrees, and the output edge is curved, with a radius of curvature of 30m. As the tilt angle decreases, the distance of the output

edge to the focal plane increases at the lower part of the focal plane, but for the upper part, the distance remains nearly unchanged. We can also find a case where the focal plane is nearly parallel the output edge, as is shown on fig 2.4a, but in this situation, it can be seen that the focal plane is too close to the output edge to be useful. By comparing focal plane lengths, it has been found that the focal plane length decreases with decreasing radius of curvature of the output edge, which is another important consideration for the cost. For example, the focal plane lengths for the designs in fig2.1b, fig2.2b, fig2.3b and fig2.4b are 7.5m, 5.9m, 4.7m and 2.3m respectively.

Fig 3 shows the resolution, dispersion and vertical image size along the focal plane as a function of the electron energy. By decreasing the tilt angle, the resolutions all become better for all radii. But for all the curved output edges, the resolution is worse than for the straight output edge. For the dispersion, the smaller the tilt angle, the larger the dispersion is, and the curved output edges are worse than the straight output edges. The vertical image size increases with decreasing the tilt angle, but this effect is not very large.

Fig 4 shows the angle Beta between an outgoing electron trajectory and the focal plane as a function of electron energy for different tilt angles. This angle has a close relationship with the path length of an electron after it exits from the exit window, so it is a very important parameter. A large angle is better for the spectrometer properties. As can be seen from Fig 4, a small tilt angle leads to a larger beta angle. The differences between different radii are very small, especially for the low analysed electron energy region.

### **3. The effect of length of DE on the spectrometer**

When the bend angle of the main beam is fixed, by increasing the length of DE, the width of the dipole magnet (size of the pole shoe transverse to the incident electron beam) and the path lengths of electrons traveled inside the magnetic field increase. This effect is equivalent to increasing the main beam bend angle, so the electron resolution is expected to be better. But, there is a shortcoming for a thicker magnet, since it causes a smaller momentum acceptance. The Gluex project requires an electron momentum acceptance from 1.2 to 9GeV/c, which imposes a limitation on the magnet pole shoe width.

For a constant magnetic field, electrons with different momentum inside the magnet have different radii of curvature. So although they enter the magnet at the same point, they will exit it at different points on the output edge. For a continuous range of analyzed electrons, these points form a continuous line on the output edge. To meet the specification on the electron momentum acceptance, at least we should make sure this line is located within the length of the output edge. Fig. 5 shows the plan view of the spectrometer. In Fig. 5, the red dashed lines on the dipole output edge show the output position for the electron momentum range from 1.2 to 9.0GeV/c. It is found, that by increasing the length of DE, the red dashed line moves towards point D. When the length of DE is 0.235m, D is

located at the end of the red dashed line. A further increase in the length of DE, moves the red dashed line outside the output edge, which results in a reduced momentum acceptance range. Hence, the length of DE should be chosen such that required range of electron momenta is analyzed by the spectrometer. Other important features shown in Fig 5 are that the focal plane length as well as the distance from the output edge to the focal plane increase by increasing DE. The distance of high-energy part of the focal plane to the main beam (outside the magnet) also increases by increasing DE. To avoid the main beam interfering with the focal plane detector, a sufficiently large distance to the main beam is necessary. From this point of view, a relatively large DE is very beneficial.

Fig 6 shows the resolution, dispersion and vertical image size as a function of the electron energy for different lengths of DE. By increasing DE, the electron energy resolution decreases, especially in the high-energy region. The dispersion and the vertical image size are also sensitive to the length of DE, both of them increasing by increasing DE. Fig 7 shows the angle beta between the analyzed electron paths and the focal plane as a function of electron energy for different lengths of DE. As can be seen from Fig 7, beta increases by increasing the length of DE, which is a positive result. So it seems that a large DE length is needed to enhance the performance of spectrometer.

#### **4. The effect of entrance angle on the spectrometer.**

Owing to the existence of the fringe field effect, when the entrance angle and exit angle are not equal to zero, the input edge and the output edge act as a thin lens, which dramatically affects the spectrometer properties. For a spectrometer, the exit angle is determined by the dipole shape, the incident electron energy and the magnetic field, but the entrance angle can be freely selected. In this section, we will study the effect of the entrance angle on the properties of the spectrometer. Following the results of sections 2 and 3, we choose the spectrometer parameters as shown in table 3.

Changing of the entrance angle only slightly changes the focal plane shape and position, when the entrance angle increases from 0 to 75 degrees, as is shown in fig 8. In Fig 9, the resolution and dispersion and vertical height as functions of electron energy are shown. It can be seen that the resolution decreases with increasing the entrance angle. The dispersion and the Beta are not very sensitive to varying the entrance angle. An obvious variation can be found in the vertical size, as is shown on fig 9c. By increasing the entrance angle, the vertical size changes dramatically in the low energy region.

Fig 10 shows the vertical beam height varying inside the magnet for different energies of energy degraded electrons. As the entrance angle is positive, the beam is vertically focused. By increasing the entrance angle, the focusing power increases. It can be seen that this affects the low-energy electrons more than the high-energy electrons.

## 5. The effect of the object distance.

As the beam energy is very high, the photon characteristic angle is small. That means the energy-degraded electrons have a small beam divergence. So even if we use a relatively large object distance, the beam spot size at the entry of the dipole will remain relatively small. That gives more flexibility to use different object distances. In this study, the object distance is varied from 1m to 10m. From fig11 and fig12, it can be seen that by increasing the object distance, the resolution decreases, the focal plane shape remains unchanged, the focal plane length becomes slightly shorter, and the distance to the output edge also becomes slightly shorter. But it should be noticed that by increasing the object distance, the beam vertical height increases. As the dipole magnet gap width is fixed, when the beam height exceeds the gap height, some of the electrons will hit the magnet pole shoe faces. Fig13 shows the vertical beam spot size at the dipole entry as a function of object size for different electron energies. It can be found that with the object distance increasing the vertical beam spot size increases monotonically. As the designed dipole magnet gap height is only 2 cm, when the object distance exceeds 6m, the vertical beam spot size exceeds this limit, which will cause part of the electrons to hit the magnet pole shoe faces. Fortunately, we can put a quadrupole before the dipole and make it focusing in the vertical plane. By using this method, the vertical height can be reduced.

## 6 The effects of a quadrupole.

One of the purposes of putting a quadrupole before the dipole is to reduce the beam vertical height to avoid electrons hitting the pole shoe faces; the other one is to meet the possible future requirement of a two-dimensional readout. To meet these requirements, the quadrupole parameters should be carefully selected, and we present details studies about the effects of varying the quadrupole parameters on the spectrometer properties to help the selection of these parameters. Owing to the high energy of the incident electron beam, the length of the quadrupole is chosen to be 0.5m, and the distance between the quadrupole and the dipole should be not less than 0.5m as we need some space to accommodate the coils of the dipole and the quadrupole.

The effects of the quadrupole tip fields on the focal plane shape and position are very small, as it can be seen from Fig 14. Fig 15 shows the vertical beam spot size for different electron energies as a function of the electron path length for different quadrupole field gradients. The six panels in the Fig 15 correspond to different quadrupole tip fields. Every panel contains 10 lines, each corresponding to different electron energies ( $x = \text{electron energy} / \text{main electron beam energy}$ ). When the quadrupole tip field is 0.5 KGs (fig 15a), the vertical height still increases with increasing the path length for  $x$  larger than 0.1, but for  $x=0.1$ , it decreases with increasing the path length. When the quadrupole tip field is 1.0 KGs, the  $x=0.2$  line begin to decrease with increasing path length. With further

increases in the quadrupole tip field, it is seen, more lines in the panels begin to decrease with increasing path length, and the magnitudes of the gradient become larger. In Fig16, the effects of a quadrupole on the resolution, dispersion, vertical size on the focal plane and the angle Beta are presented. It can be seen that by increasing the quadrupole field gradient, the resolution slightly decreases. The dispersion and the Beta are not affected by the quadrupole. The vertical size at the focal plane is the parameter most sensitive to the tip field of quadrupole, making it possible to choose a suitable tip field to obtain a suitable vertical size.

## 7. Parameter selection for the spectrometer.

To optimize the design of a good spectrometer magnet, there are many things that should be considered, such as resolution, dispersion and vertical height at focal plane or/and inside the magnet. The focal plane shape and length, and its separation from the magnet and the main beam are also important. In order to optimize the resolution, from Fig 3 and Fig 6, it seems we need to use a smaller tilt angle and a longer length for DE which defines the width of the pole shoes. However, too small a tilt angle gives a very complicated focal plane shape, which will cause difficulties in the construction of the focal plane detector. On the other hand, a small tilt angle and a large DE increase the separation between the focal plane and the output edge, as well as increasing the length of the focal plane. So when we select the spectrometer parameters, we need to make a compromise between the resolution and the focal plane length, shape, and the output edge focal plane separation. We also find that a curved output edge gives a much shorter focal plane, which could reduce the cost of the construction, but give a poorer resolution. In section 4 we show that a large object distance is very beneficial for the resolution and has little effect on the focal plane shape and position, but due to the space we still have to choose a relatively small object distance. The entrance angle also has some positive effects on the spectrometer properties. Since the effects of the second order aberrations have yet to be studied, we have chosen 0 degrees as the entrance angle. After a systematic study of second order aberrations we may choose a more suitable entrance angle.

The Gluex Project requires a photon resolution of 0.1 % $E_0$  r.m.s in the photon energy range of 8~9 GeV (from CDR report version 4). Considering the electron beam energy spread of 0.08%  $E_0$  r.m.s., the electron energy resolution should be at least 0.06 % $E_0$  r.m.s. A nearly straight focal plane is also required for this project. (It should be mentioned that the r.m.s. energy resolution is a different definition from the definition of the energy resolution often used in the literature

of magnet optics[3], ie  $R = \frac{A\omega}{D}$ . In the CDR report, the r.m.s. energy resolution refers to the standard deviation of the energy, which is much smaller than the standard energy resolution. Compared with the energy resolution definition in section 1, the r.m.s. energy resolution is equal to 1/2 of the resolution defined in section 1.) To meet the requirements of the Gluex project, a group of parameters

have been selected as shown in table 4. In the current situation, the small bend angle and the large beam spot size result in a rather poor resolution. When the object distance is 1.5m, the resolution just satisfies the requirement of Gluex. But if the object distance is 3m, the resolution will become much better, and even a curved output edge can be considered.

Fig 17 shows the geometry plan view of some possible final designs. Fig 18 shows the resolution, dispersion, vertical image size and the angle Beta for these designs. Due to the small object distance, the vertical height inside the dipole is much less than the magnet gap height. So it is not shown here. Some important parameters and the TRANSPORT results are shown in table 5 and table 6 for the curved and straight output edge cases. In order to compare it with the CDR results, the resolution used here follows the r.m.s. definition. The effect of a quadrupole is also considered in the design. The quadrupole parameters were chosen to minimize the contribution from the beam spot size on the vertical beam height at the focal plane at around 9 GeV/c electron momentum.

## **8 Conclusion**

By using the computer code TRANSPORT, the tilt angle and the radius of curvature of the output edge, the magnet pole shoe width, the object distance, the beam entrance angle, and having a quadrupole before the dipole were varied. The effects on the resolution, dispersion, beam vertical spot size and other properties have been systematically studied. Possible magnet parameters have been selected. These possible designs meet the requirements for the resolution specified in the CDR.

### References:

- [1] R. T. Jones, Hall D Conceptual Design Report, v4.0 September 25 2002
- [2] J. D. Kellie, I. Anthony, S. J. Hall, I. J. D. Macgregor, A. Mcpherson et al. Nuclear Instrument and Methods in Physics Research A241 (1985)153-168
- [3] Livingood, The Optics of Dipole Magnets, Academic Press New York and London, 1969

Table 1 Main electron beam properties

<i>Parameters</i>	<i>properties</i>
Transverse spot size at radiator $\Delta x$	1.7mm r.m.s.
Vertical spot size at radiator $\Delta y$	0.5 mm r.m.s.
Transverse beam divergence $\Delta x'$	0.020 mr r.m.s.
Vertical beam divergence $\Delta y'$	0.005 mr r.m.s.
r.m.s. energy spread $\Delta E/E_0$	0.080 % r.m.s.

Table 2 Scattered electron beam properties

<i>Parameters</i>	<i>properties</i>
Transverse spot size at radiator x	6.8mm
Vertical spot size at radiator y	2.0mm
Transverse beam divergence x'	$4mc(E_0-E)/E_0E$ .
Vertical beam divergence y'	$4mc(E_0-E)/E_0E$

Table 3 Selected spectrometer parameters.

<i>Parameters</i>	<i>properties</i>
Transverse spot size at radiator x	6.8mm
Vertical spot size at radiator y	2.0mm
Transverse beam divergence x'	$4mc(E_0-E)/E_0E$
Vertical beam divergence y'	$4mc(E_0-E)/E_0E$
Tilt angle	84.2 degree
Radius of curvature	infinite
Length of DE	0.188m
Object distance	2 m
Entrance angle	0—75 degree

Table 4 The possible parameters selected for the final designs.

<i>Parameters</i>	<i>properties</i>
Transverse spot size at radiator x	6.8mm
Vertical spot size at radiator y	2.0mm
Transverse beam divergence x'	$4mc(E_0-E)/E_0E$
Vertical beam divergence y'	$4mc(E_0-E)/E_0E$
Tilt angle	84.0 or 87.5degree
Radius of curvature	infinite or 50m
Length of DE	0.188m
Object distance	3 m
Entrance angle	0 degree

Table 5, Geometrical parameters of the tagging spectrometers.  
 Bend =deflection angle; Drift=distance from exit edge to focal plane;  
 Angle=angle between electron path and focal plane;  
 cm/%E<sub>0</sub>=dispersion in units of per percent of the incident energy

Curved output edge, without quadrupole

k (GeV)	Bend (deg)	Drift (m)	Angle (deg)	cm/%E <sub>0</sub> perp. to ray	cm/%E <sub>0</sub> along FP
6	15.551	24678	6.021	0.987	9.405
7	15.697	2.2659	6.968	1.131	9.323
8	16.165	2.0211	8.119	1.343	9.510
9	17.156	1.7231	9.647	1.685	10.053
10	19.209	1.3541	12.024	2.335	11.207
11	24.525	0.8705	17.011	4.135	14.134

Curved output edge, with quadrupole

k (GeV)	Bend (deg)	Drift (m)	Angle (deg)	cm/%E <sub>0</sub> perp. to ray	cm/%E <sub>0</sub> along FP
6	15.551	2.5616	6.162	0.987	9.195
7	15.697	2.3786	7.191	1.138	9.089
8	16.165	2.1546	8.453	1.362	9.266
9	17.156	1.8776	10.134	1.729	9.829
10	19.209	1.5260	12.721	2.443	11.092
11	24.525	1.0407	17.905	4.473	14.550

Straight output edge without quadrupole

k (GeV)	Bend (deg)	Drift (m)	Angle (deg)	cm/%E <sub>0</sub> perp. to ray	cm/%E <sub>0</sub> along FP
6	17.867	3.5887	6.876	1.615	13.492
7	18.379	3.0524	7.400	1.745	13.546
8	19.105	2.5165	8.141	1.934	13.655
9	20.226	1.9781	9.272	2.238	13.891
10	22.219	1.4297	11.242	2.818	14.454
11	27.043	0.8442	15.754	4.420	16.281

Straight output edge with quadrupole

k (GeV)	Bend (deg)	Drift (m)	Angle (deg)	cm/%E <sub>0</sub> perp. to ray	cm/%E <sub>0</sub> along FP
6	17.867	3.7419	6.958	1.629	13.450
7	18.379	3.2092	7.503	1.764	13.513
8	19.105	2.6759	8.276	1.963	13.639
9	20.226	2.1385	9.459	2.286	13.909
10	22.219	1.5866	11.521	2.910	14.568
11	27.043	0.9839	16.187	4.669	16.750

Table 6, Optical properties and resolutions of the tagging spectrometers.

(x x), (y y) and (y y') = the first order matrix element where x and y are radial and transverse coordinates respectively.

$\Delta k_{\text{beam}}$  = r.m.s energy resolution due to beam energy uncertainty

$\Delta k_{\text{spot}}$  = r.m.s energy resolution due to beam spot size

$\Delta k_{\text{tot}}$  = total r.m.s energy resolution except detector size

$\Delta y_{\text{tot}}$  = transverse r.m.s position resolution due to spot size on radiator

$\Delta y_{\text{chara}}$  = transverse r.m.s size correspond to one characteristic electron angle :  $(m/E_0)(k/(E_0-k))$

Curved output edge, radius of curvature 50 m  
without quadrupole

k (GeV)	(x x) (mm/mm)	(y y) (mm/mm)	(y y') (mm/mr)	$\Delta k_{\text{beam}}$ (E <sub>0</sub> %)	$\Delta k_{\text{spot}}$ (E <sub>0</sub> %)	$\Delta k_{\text{total}}$ (E <sub>0</sub> %)	$\Delta y_{\text{total}}$ (cm)	$\Delta y_{\text{chara}}$ (cm)
6	-0.382	2.344	17.992	0.080	0.066	0.104	1.172	0.750
7	-0.384	2.342	16.425	0.080	0.058	0.099	1.171	0.958
8	-0.377	2.327	14.841	0.080	0.048	0.093	1.163	1.237
9	-0.356	2.293	13.184	0.080	0.036	0.088	1.146	1.648
10	-0.315	2.228	11.359	0.080	0.023	0.083	1.114	2.366
11	-0.238	2.083	9.104	0.080	0.010	0.080	1.041	4.173

With quadrupole (length=50cm, pole tip field=-2.95KGauss, Radius of aperture 5 cm)

6	-0.324	0.497	14.158	0.080	0.056	0.098	0.248	0.590
7	-0.321	0.399	12.427	0.080	0.048	0.093	0.199	0.725
8	-0.309	0.237	10.565	0.080	0.039	0.089	0.154	0.880
9	-0.282	-0.036	8.422	0.080	0.028	0.085	0.018	1.053
10	-0.234	-0.547	5.645	0.080	0.016	0.082	0.273	1.176
11	-0.148	-1.783	0.941	0.080	0.006	0.080	0.891	0.431

Straight output edge  
Without quadrupole

k (GeV)	(x x) (mm/mm)	(y y) (mm/mm)	(y y') (mm/mr)	$\Delta k_{\text{beam}}$ (E <sub>0</sub> %)	$\Delta k_{\text{spot}}$ (E <sub>0</sub> %)	$\Delta k_{\text{total}}$ (E <sub>0</sub> %)	$\Delta y_{\text{total}}$ (cm)	$\Delta y_{\text{chara}}$ (cm)
6	-0.516	2.456	21.175	0.080	0.054	0.097	1.228	0.882
7	-0.480	2.415	18.911	0.080	0.047	0.093	1.207	1.103
8	-0.438	2.365	16.629	0.080	0.039	0.089	1.182	1.386
9	-0.386	2.302	14.308	0.080	0.029	0.085	1.156	1.788
10	-0.321	2.215	11.895	0.080	0.019	0.082	1.107	2.478
11	-0.229	2.064	9.201	0.080	0.009	0.080	1.032	4.217

With quadrupole (length=50cm, pole tip field=-2.58KGauss, Radius of aperture 5 cm)

6	-0.448	0.463	17.154	0.080	0.047	0.093	0.231	0.715
7	-0.410	0.357	14.756	0.080	0.040	0.089	0.178	0.861
8	-0.365	0.208	12.261	0.080	0.032	0.086	0.104	1.022
9	-0.310	-0.020	9.577	0.080	0.023	0.083	0.010	1.197
10	-0.241	-0.425	6.450	0.080	0.014	0.081	0.213	1.344
11	-0.146	-1.407	1.855	0.080	0.005	0.080	0.704	0.850

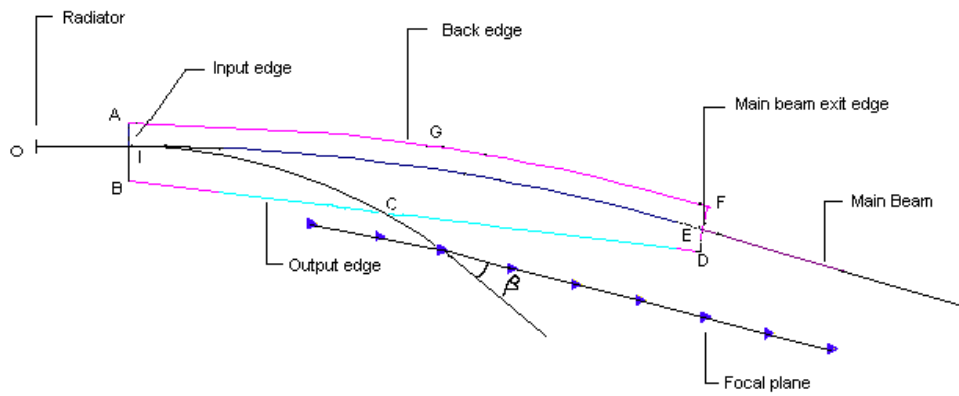


Fig. 1 Plan view of the tagging spectrometer from above.

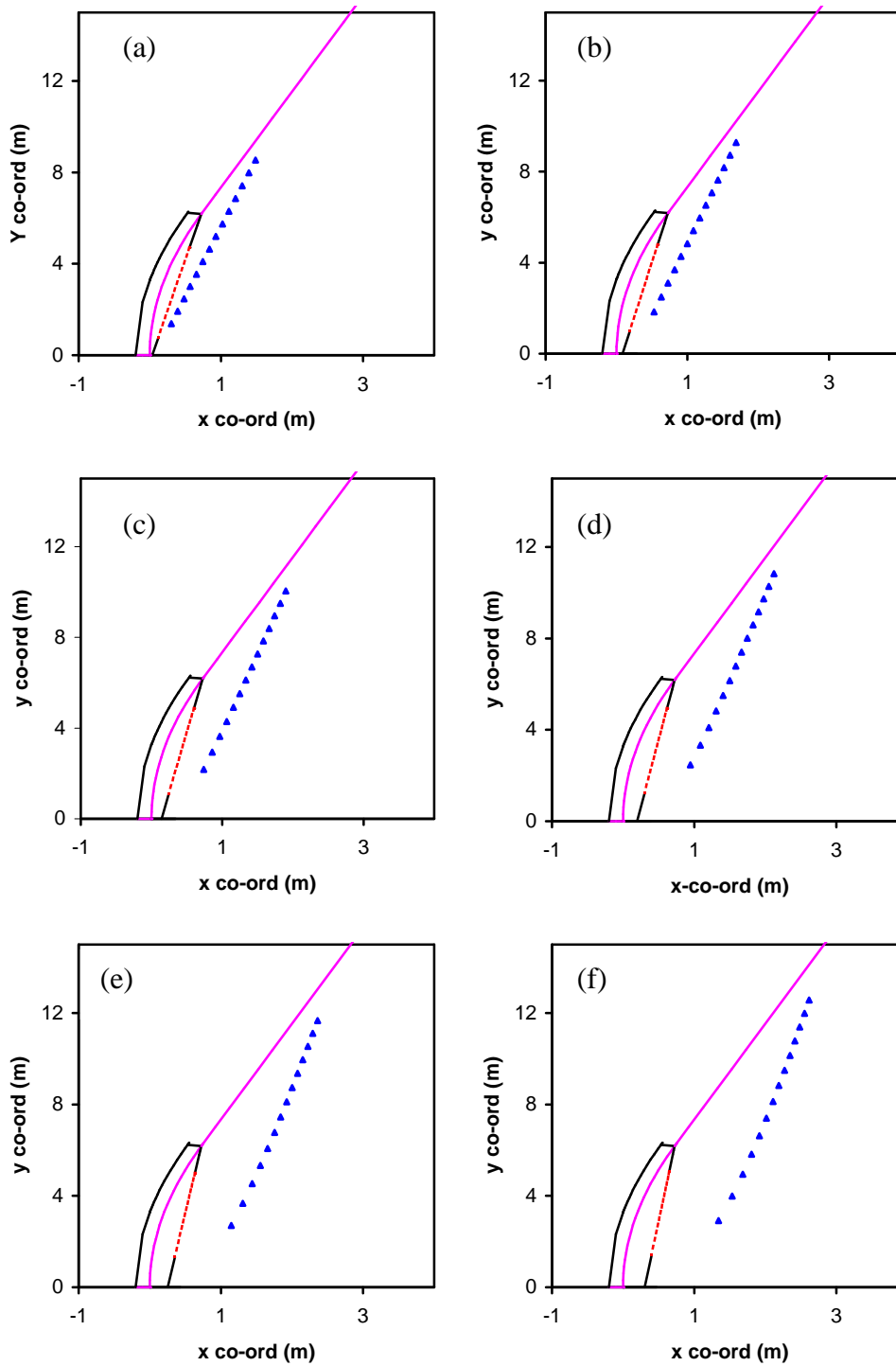


Fig 2.1 Focal plane position (shown by the blue triangles) corresponding to the different geometrical structure of the magnet. (output edge is straight, from (a) to (e) the tilt angle varies from 83 to 80.5 degree, step  $-0.5$  degree)

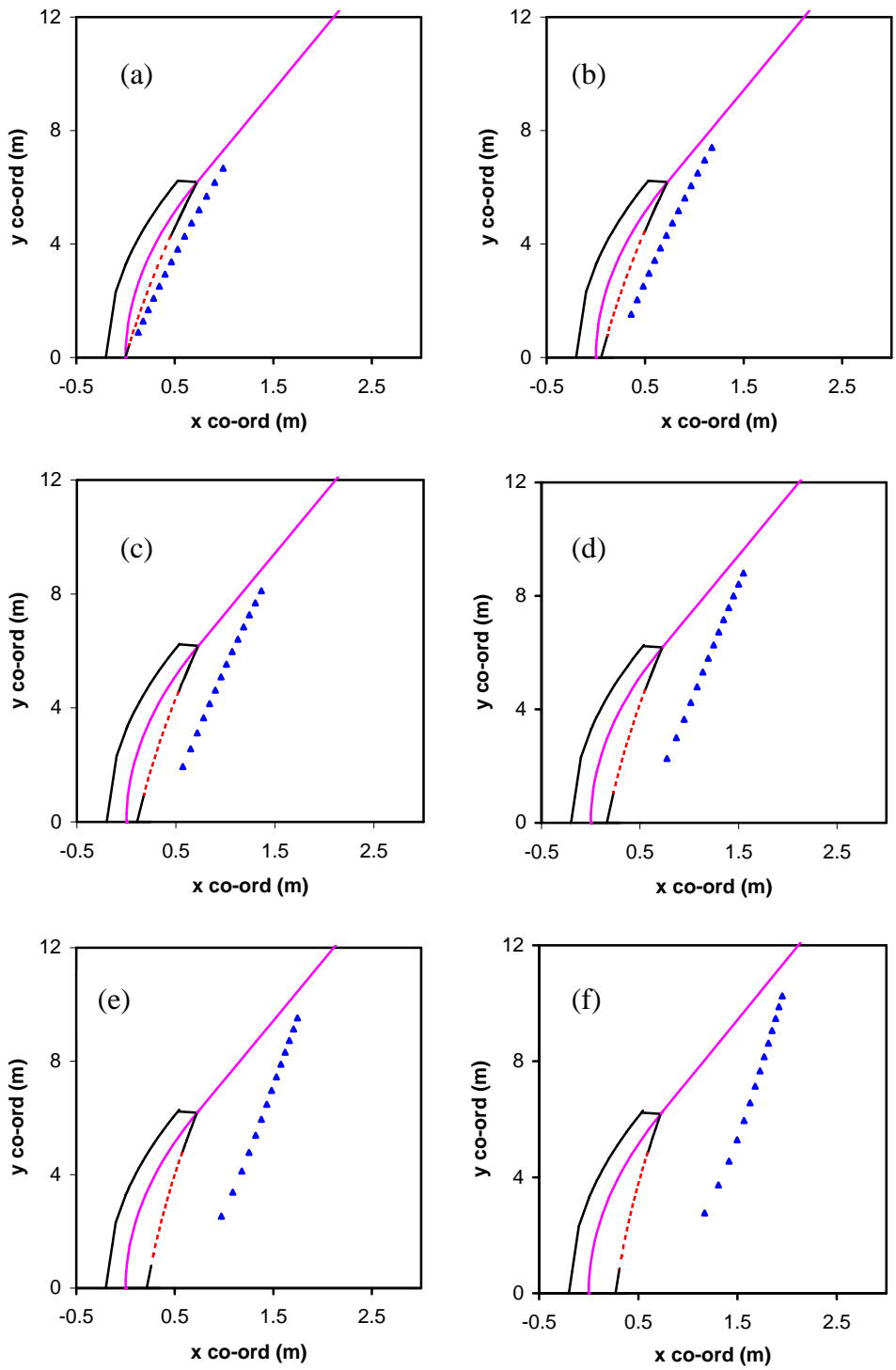


Fig 2.2 Focal plane position (shown by the blue triangles) corresponding to the different magnet geometries. (output edge is curved, radius of curvature 100m, from (a) to (e) the tilt angle varies from 85 to 82.5 degree, step  $-0.5$  degree)

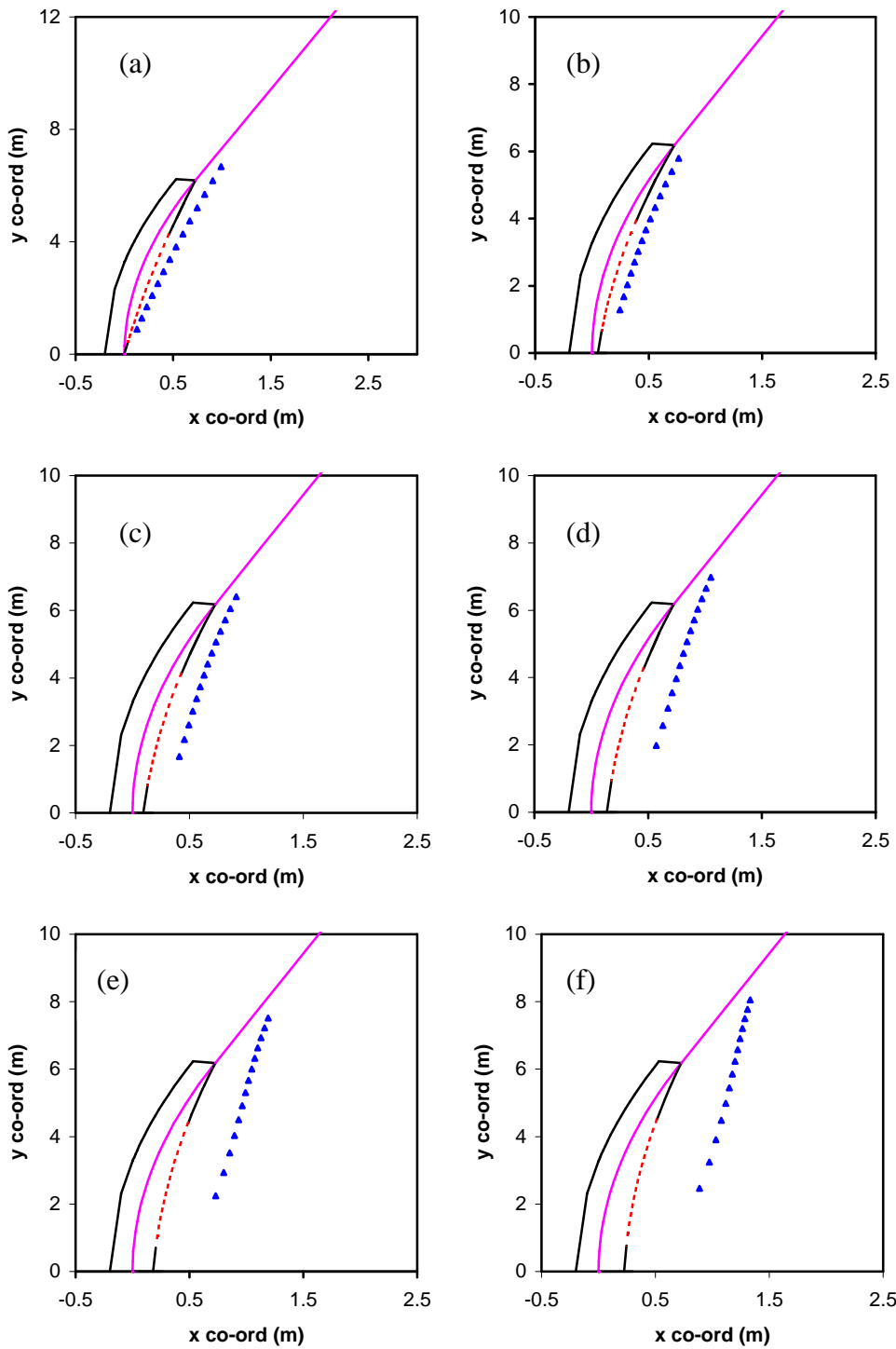


Fig 2.3 Focal plane position (shown by the blue triangles) corresponding to the different magnet geometries. (output edge is curved, radius of curvature 50m, from (a) to (e) the tilt angle varies from 86.8 to 84.8 degree, step  $-0.4$  degree)

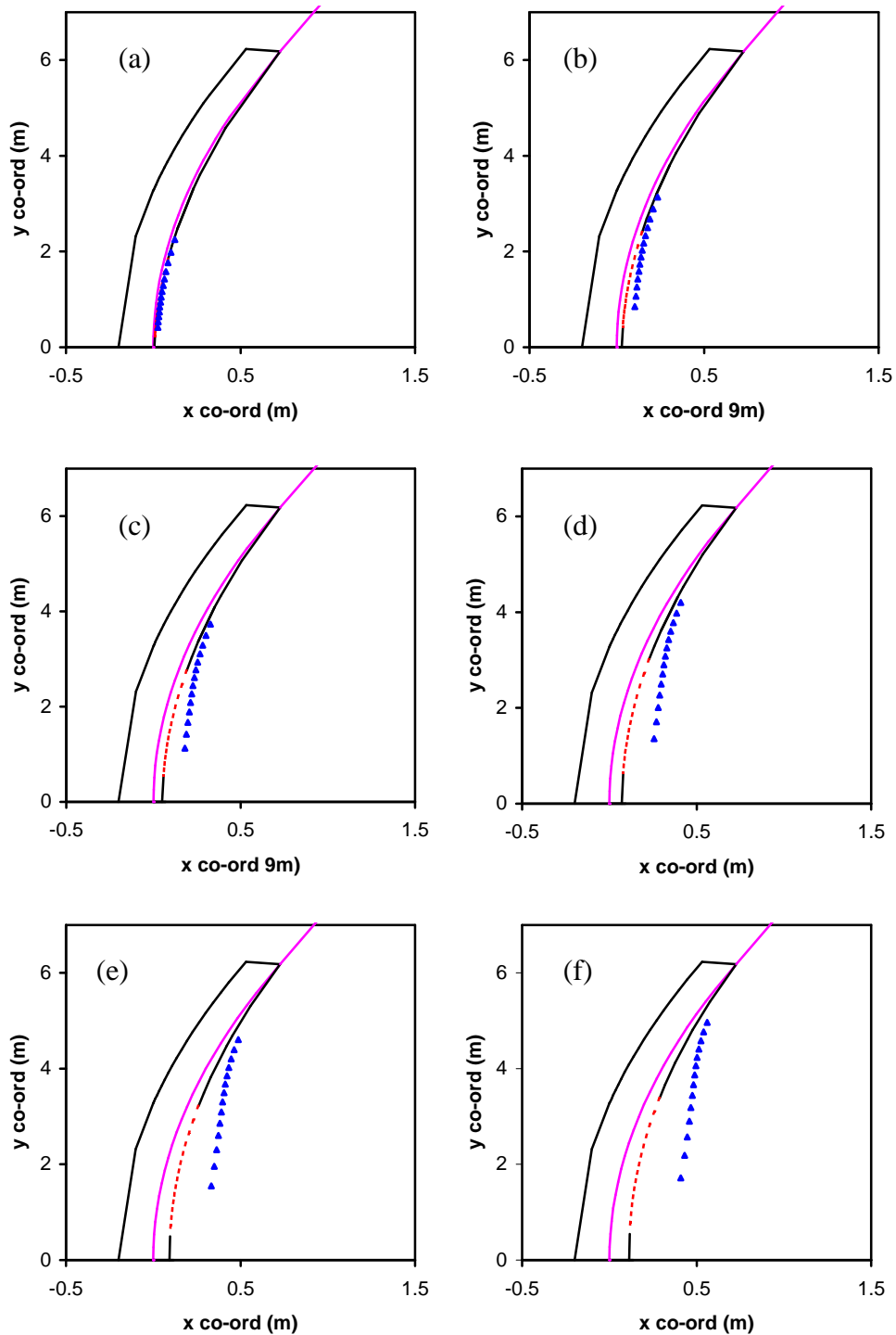


Fig 2.4 Focal plane position (shown by the blue triangles) corresponding to the different geometrical structure of the magnet. (output edge is curved, radius of curvature 30m, from (a) to (e) the tilt angle varies from 89.2 to 88.2 degree, step – 0.2 degree)

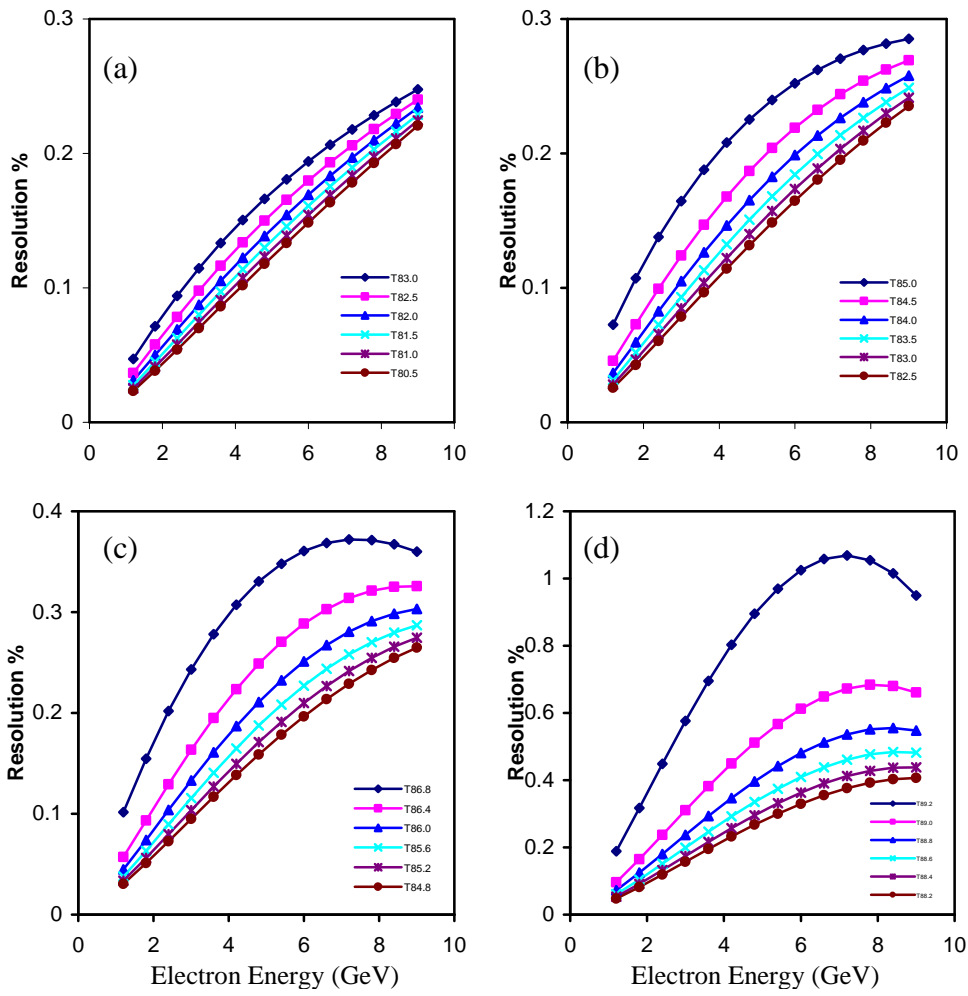


Fig 3.1 Electron resolution vs. the electron energy for different tilt angles and different radii. (a: straight, b:100 m, c: 50m, d 30 m)

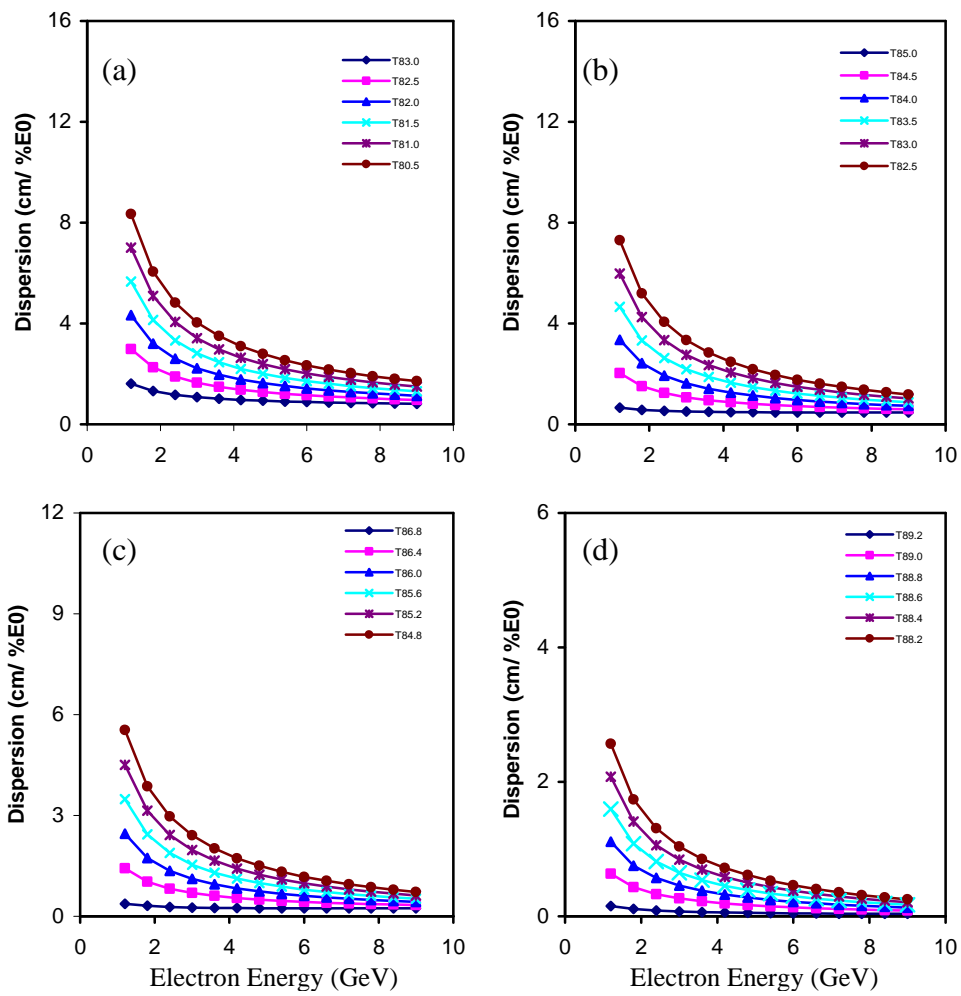


Fig 3.2 Dispersion vs. the electron energy for different tilt angles and different radii. (a: straight, b:100 m, c: 50m, d 30 m)

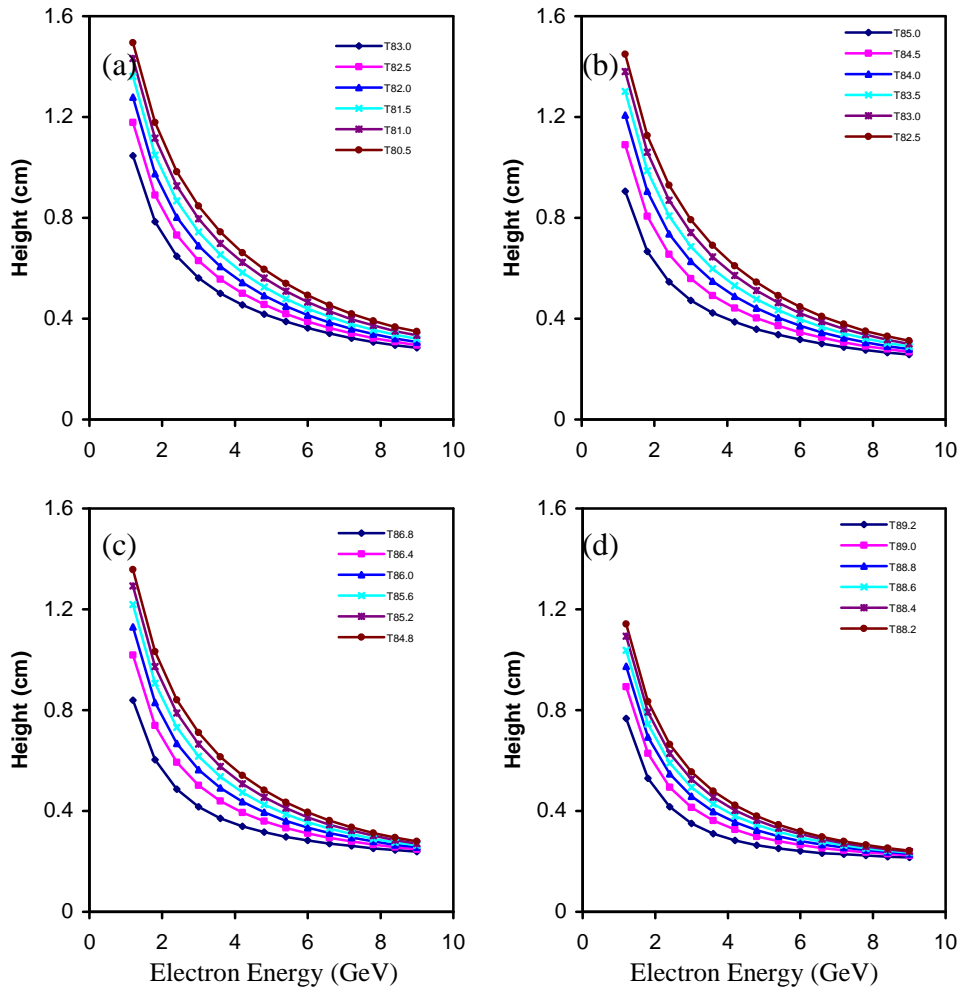


Fig 3.3 Vertical image size on the focal plane vs. the electron energy for different tilt angles and different radii. (a: straight line, b:100 m, c: 50m, d 30 m)

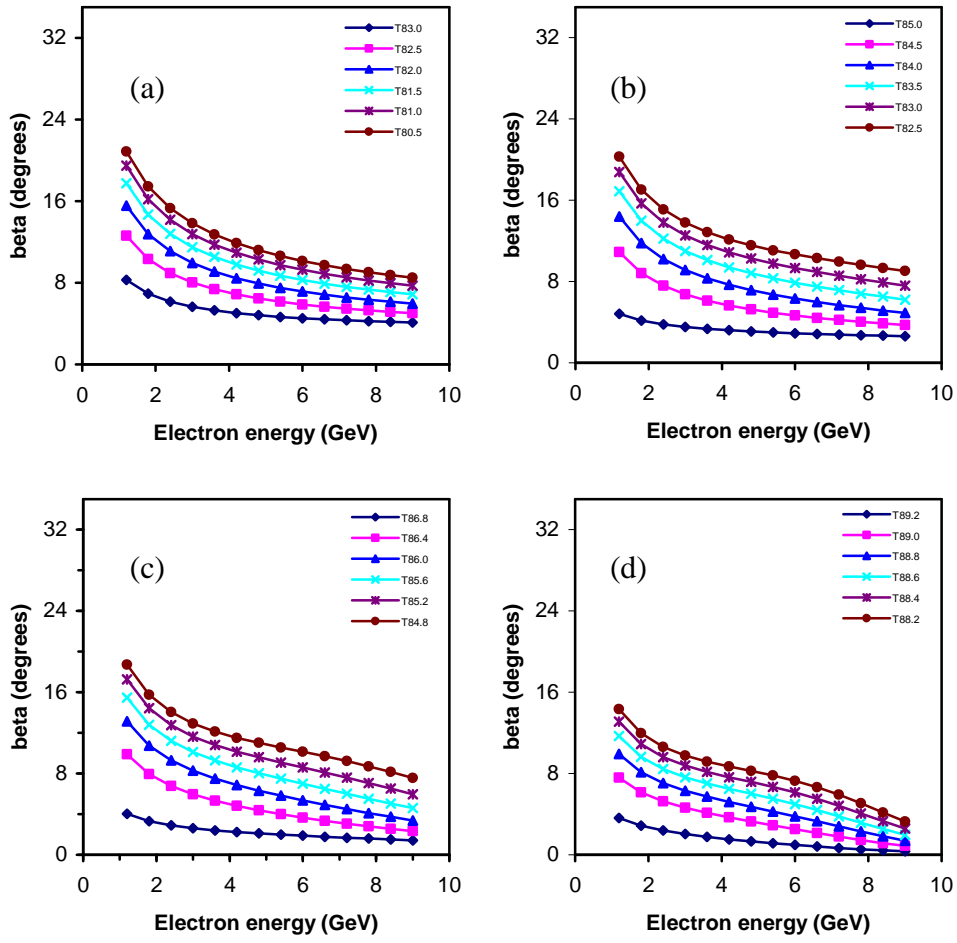


Fig 4. Angle beta between an outgoing electron path and the focal plane vs. electron energy for different tilt angles. (a: straight, b:100 m, c: 50 m, d 30 m)

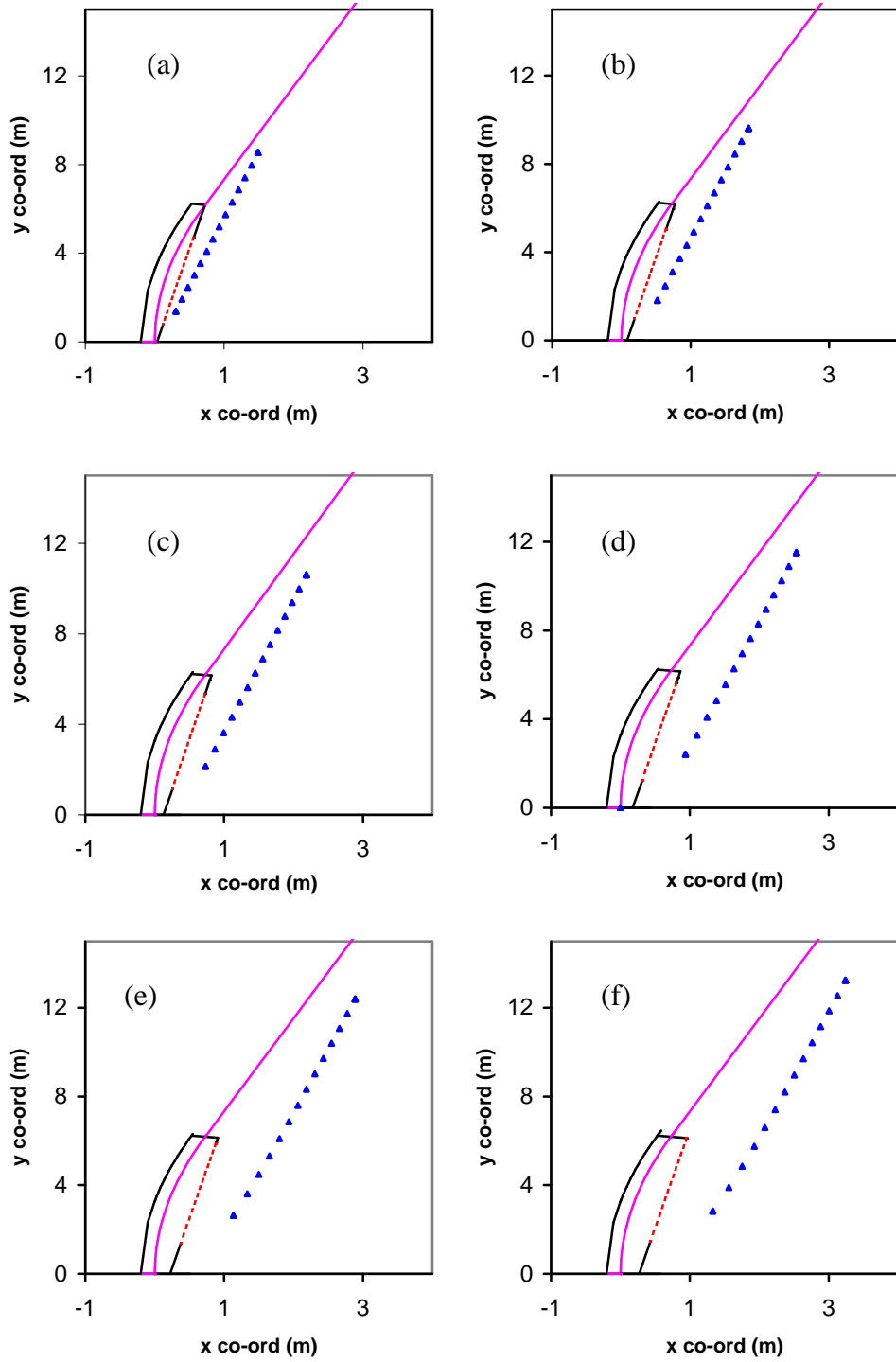


Fig. 5 The geometry plan view of the spectrometer for different magnet thicknesses. (a: DE=0.0m, b: DE=0.047m,c:DE=0.094m;d:DE=0.141m,e:DE=0.188m,f:DE=0.235m)

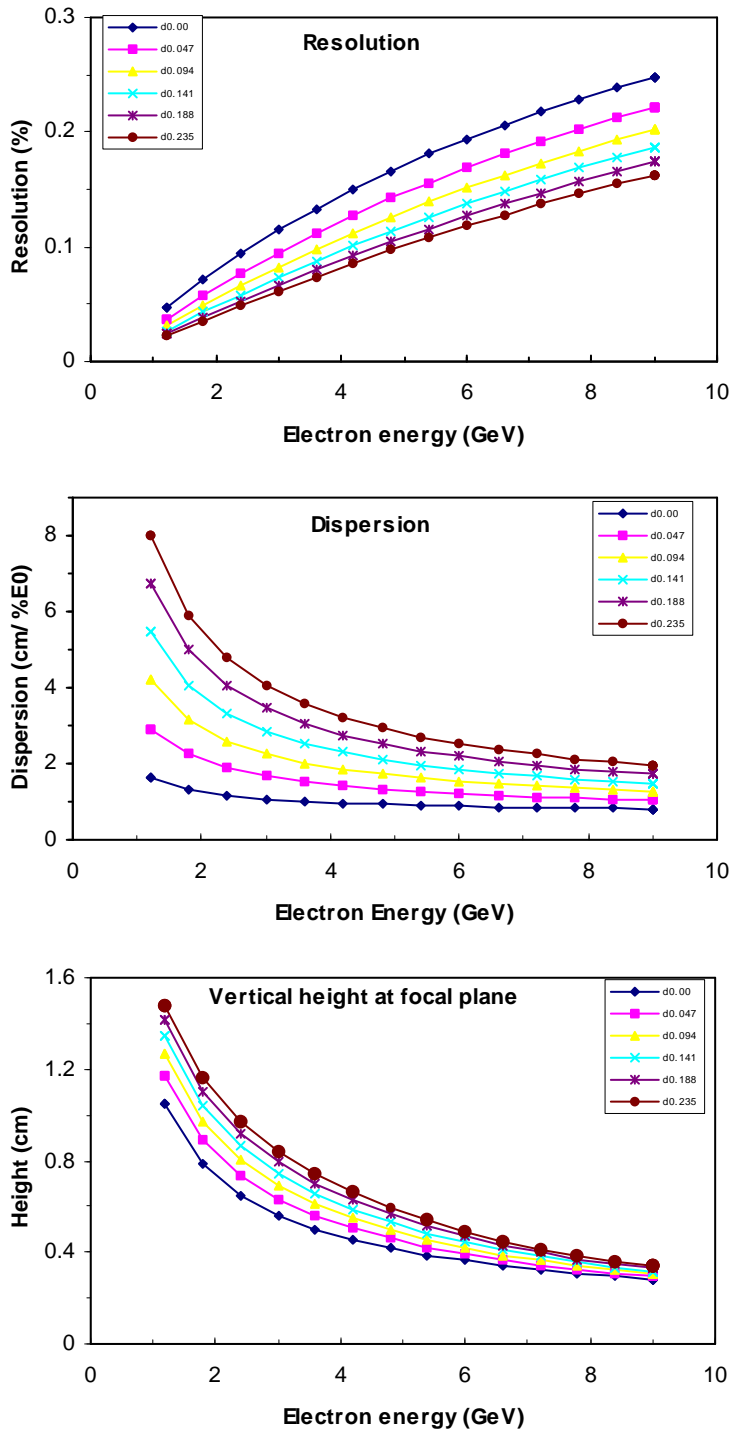


Fig6. Resolution, dispersion and vertical image size at the focal plane vs. electron energy for different magnet thicknesses.

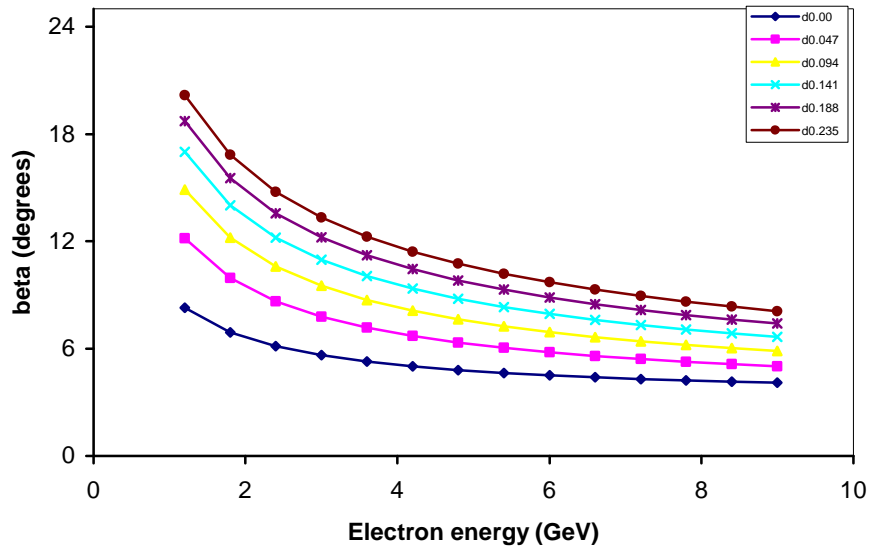


Fig 7 Angle between the electron path and focal plane vs. electron energy for different magnet thicknesses.

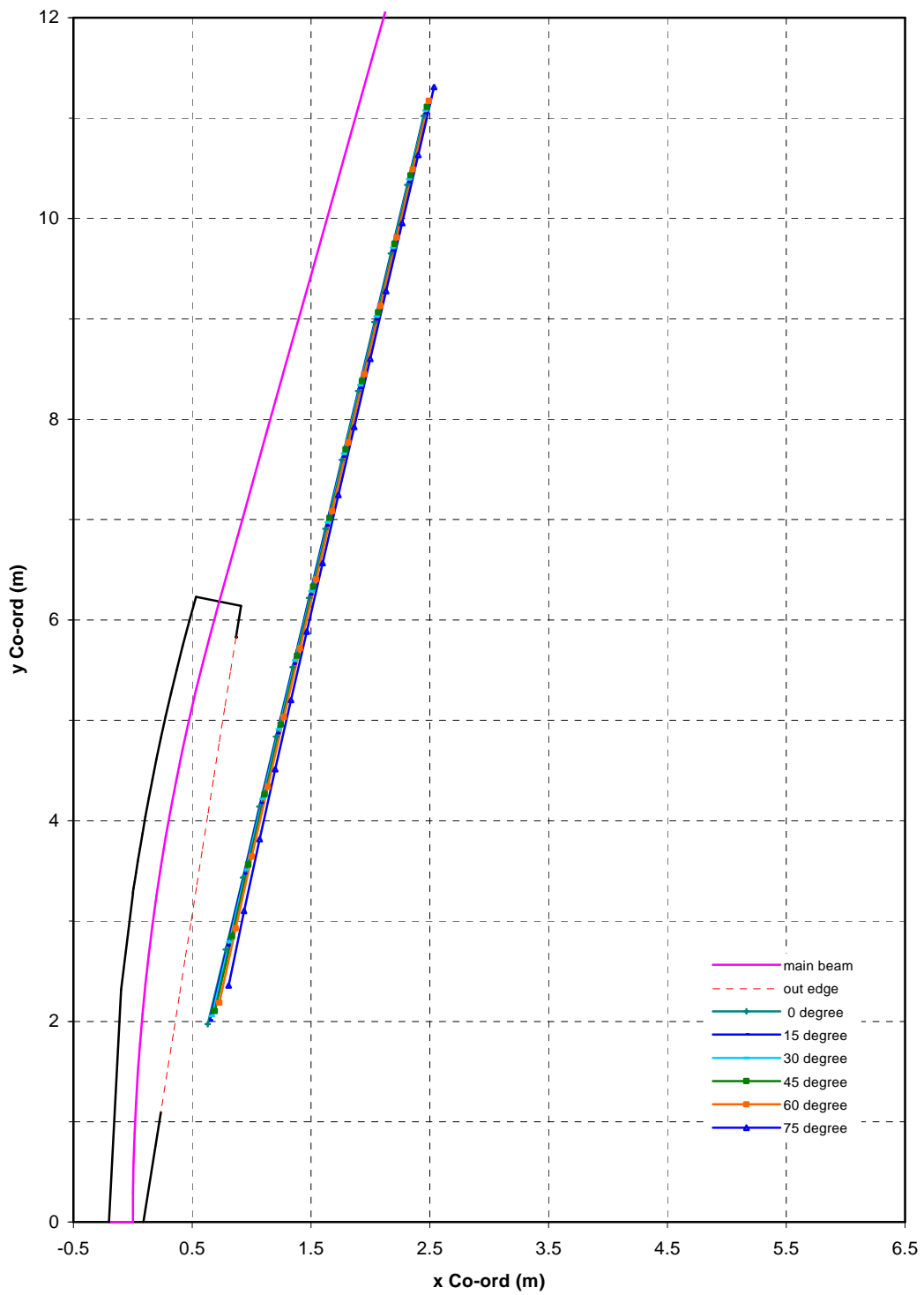


Fig 8 Plan view of the spectrometer magnet and the focal plane position for different entrance angles.

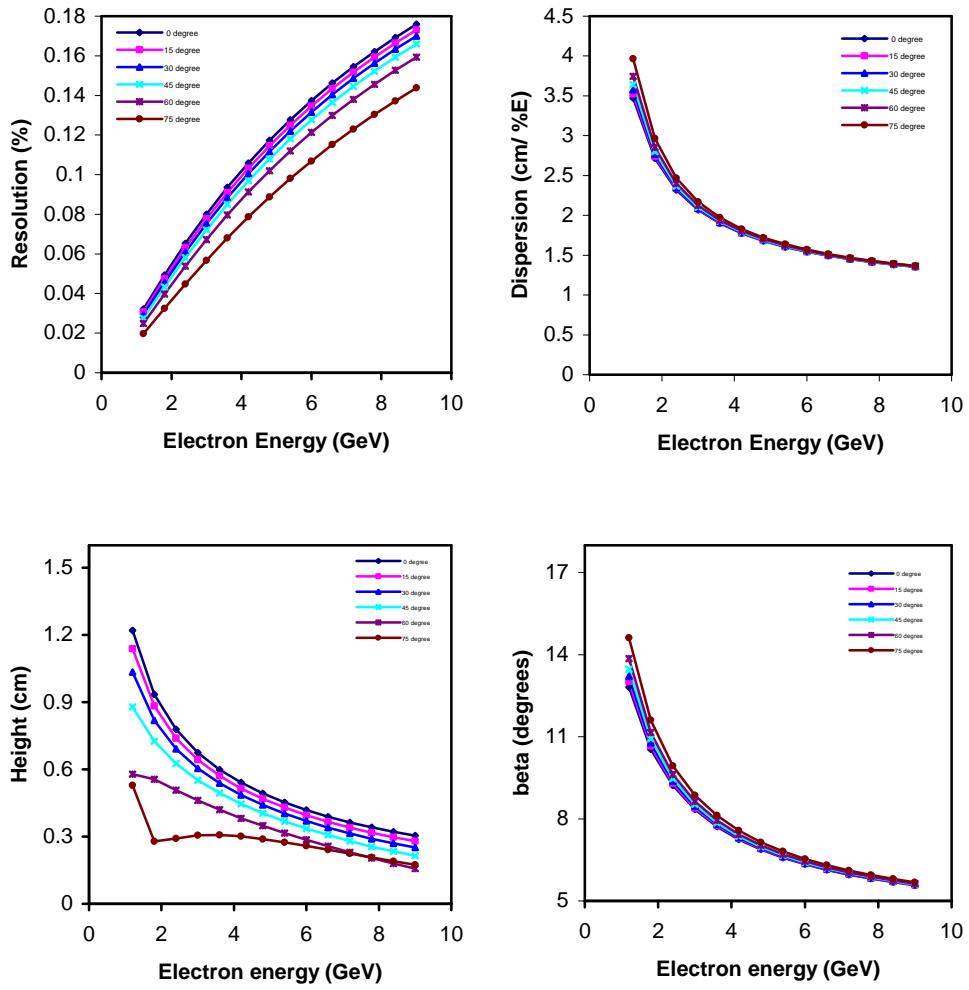


Fig 9. Resolution, dispersion, vertical height and Beta as a functions of the electron energy for different entrance angles.

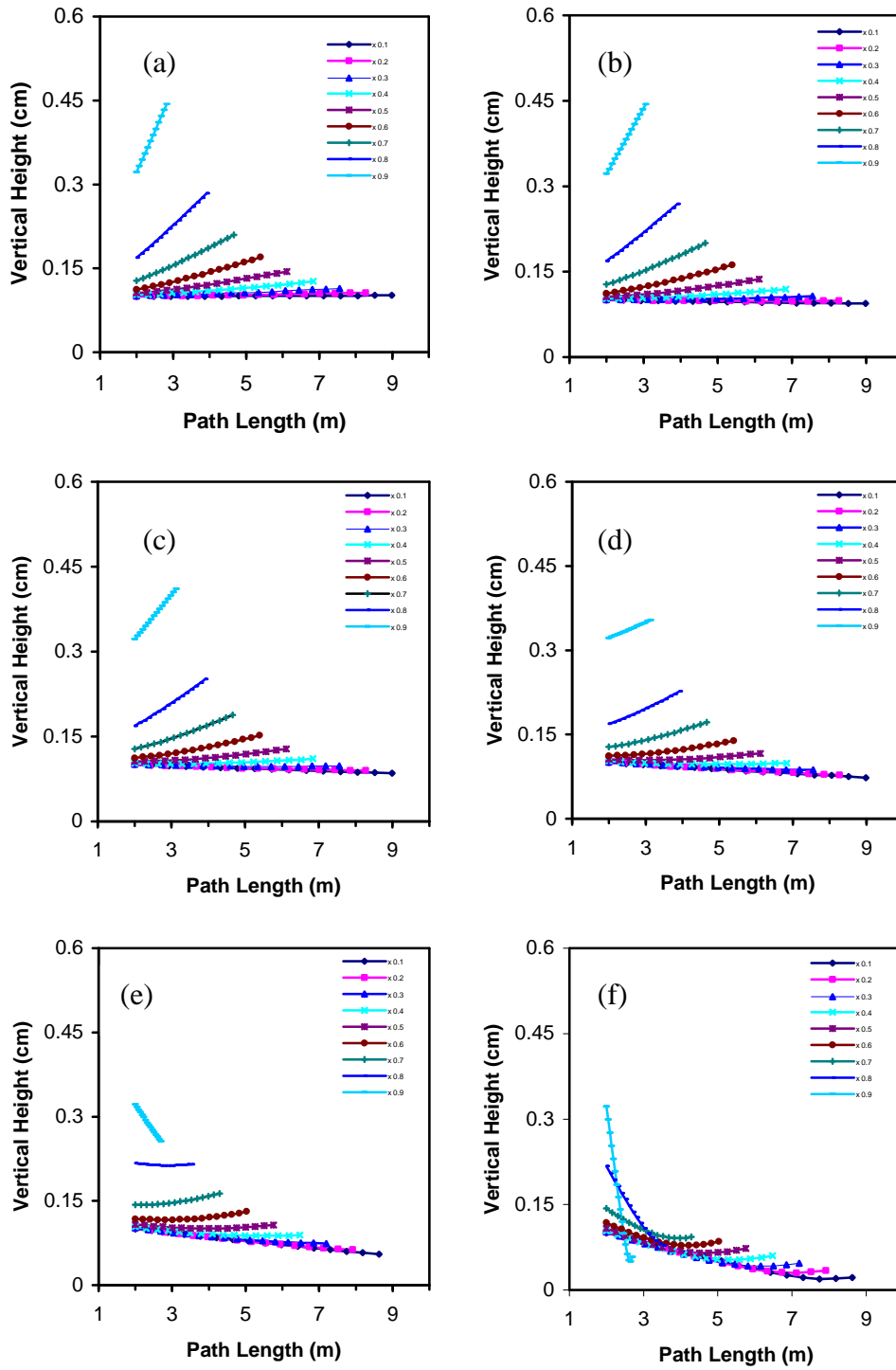


Fig 10 Beam vertical height inside the magnet for different entrance angles (a:0 degree, b:15 degree, c:30 degree, d:45 degree, e:60 degree f:75 degree)

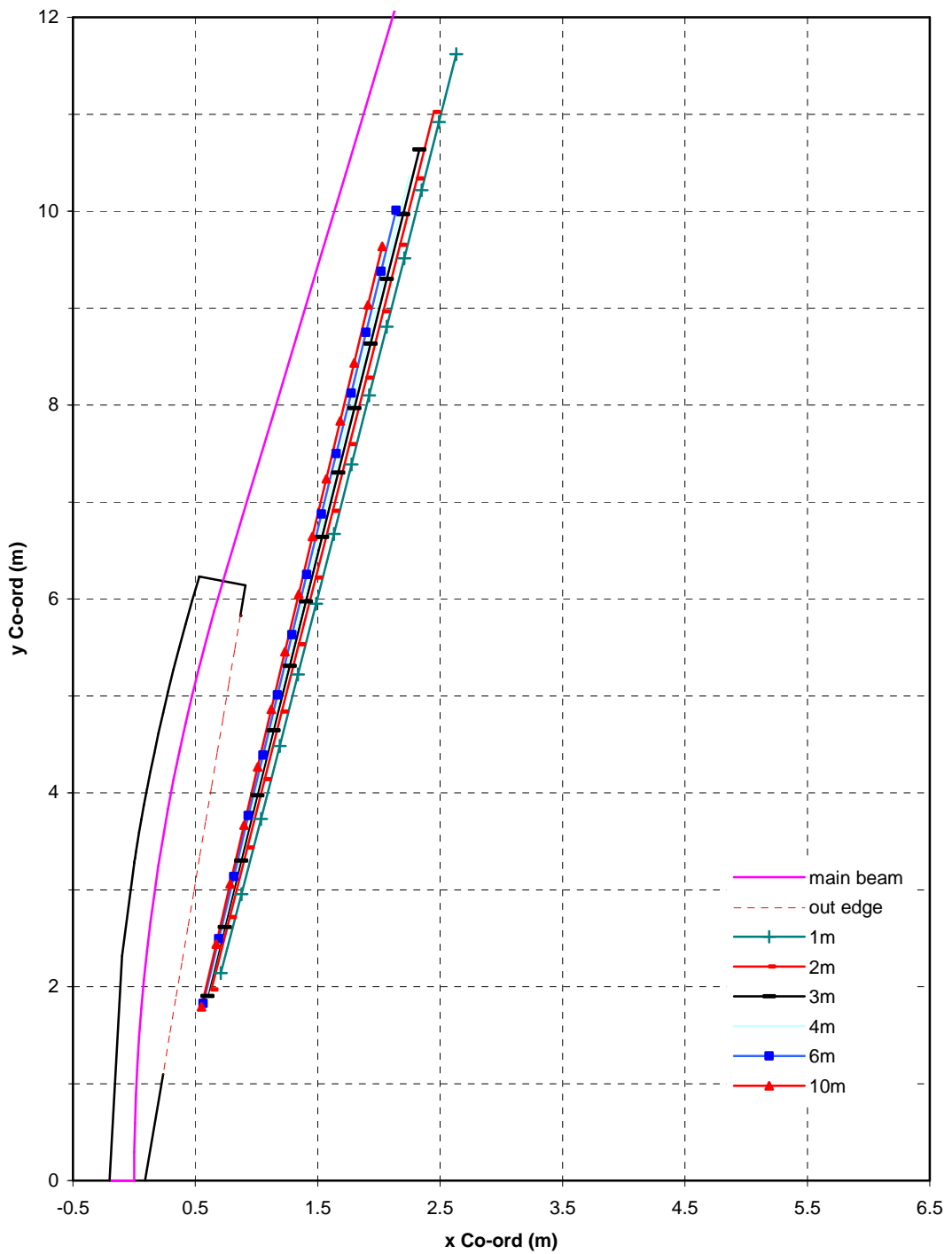


Fig 11 Plan view of magnet geometry and focal plane positions for different object Distances.

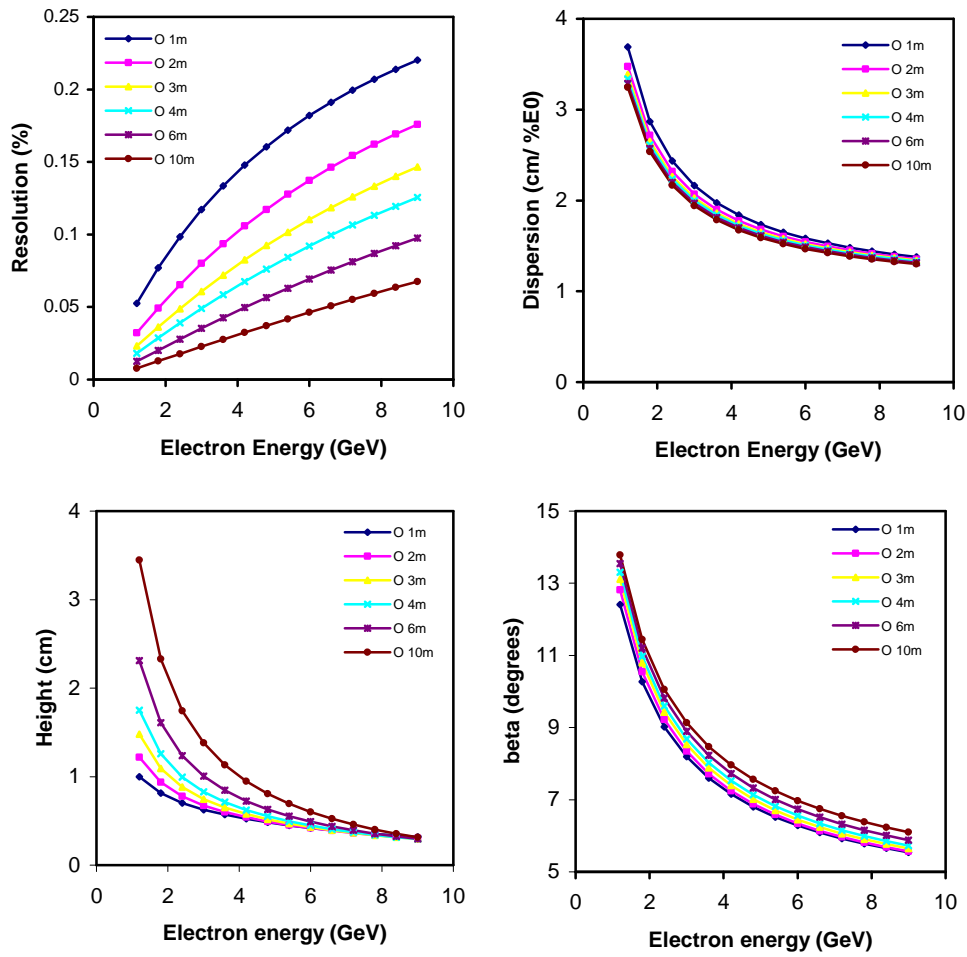


Fig 12 Resolution, dispersion, vertical height, and Beta as a function of electron energy for different object distances.

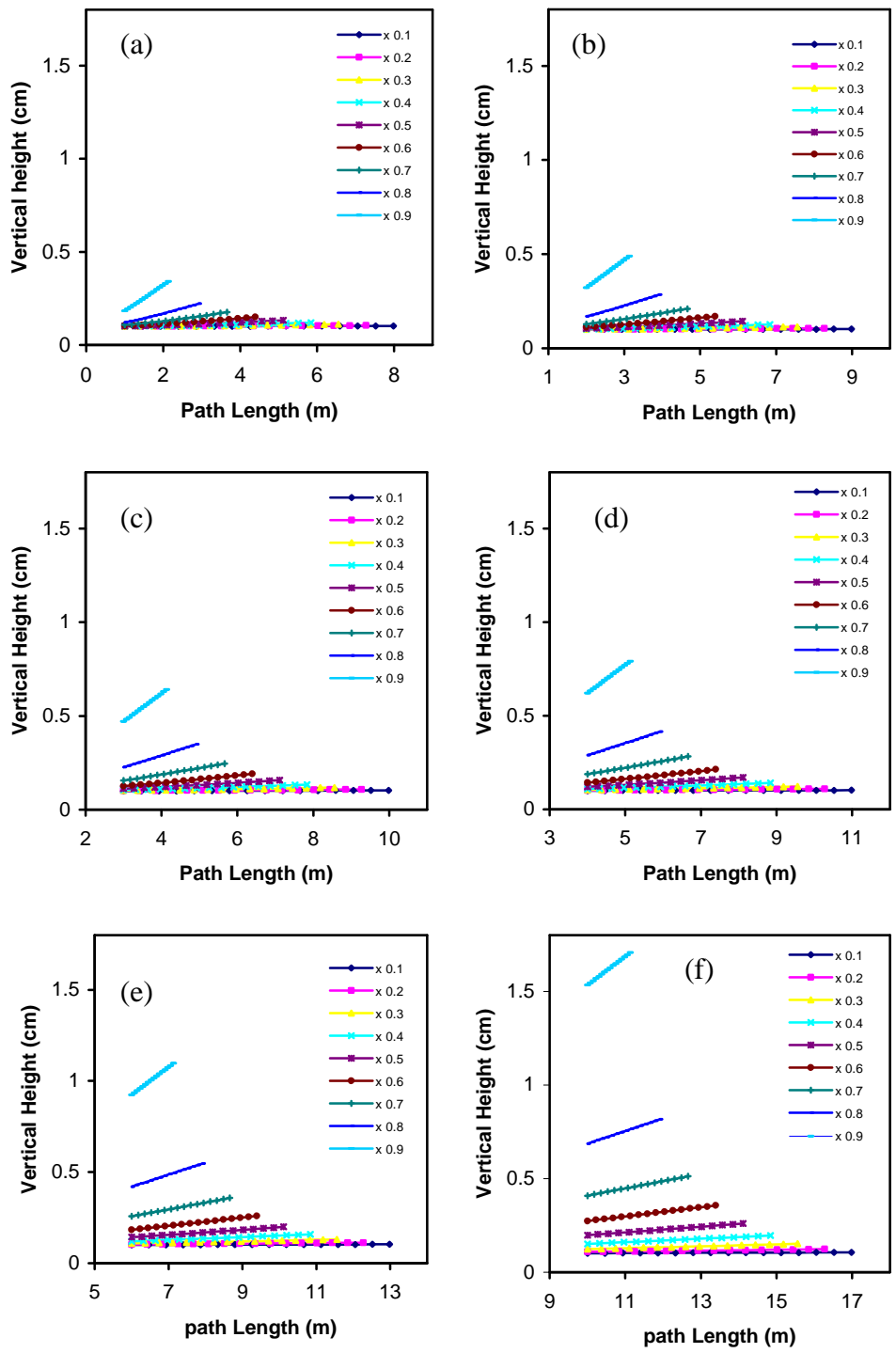


Fig 13 Beam vertical height inside the magnet for different object distances.  
(a: 1m, b:2m,c:3m,d:4m,e:6m,f:10m)

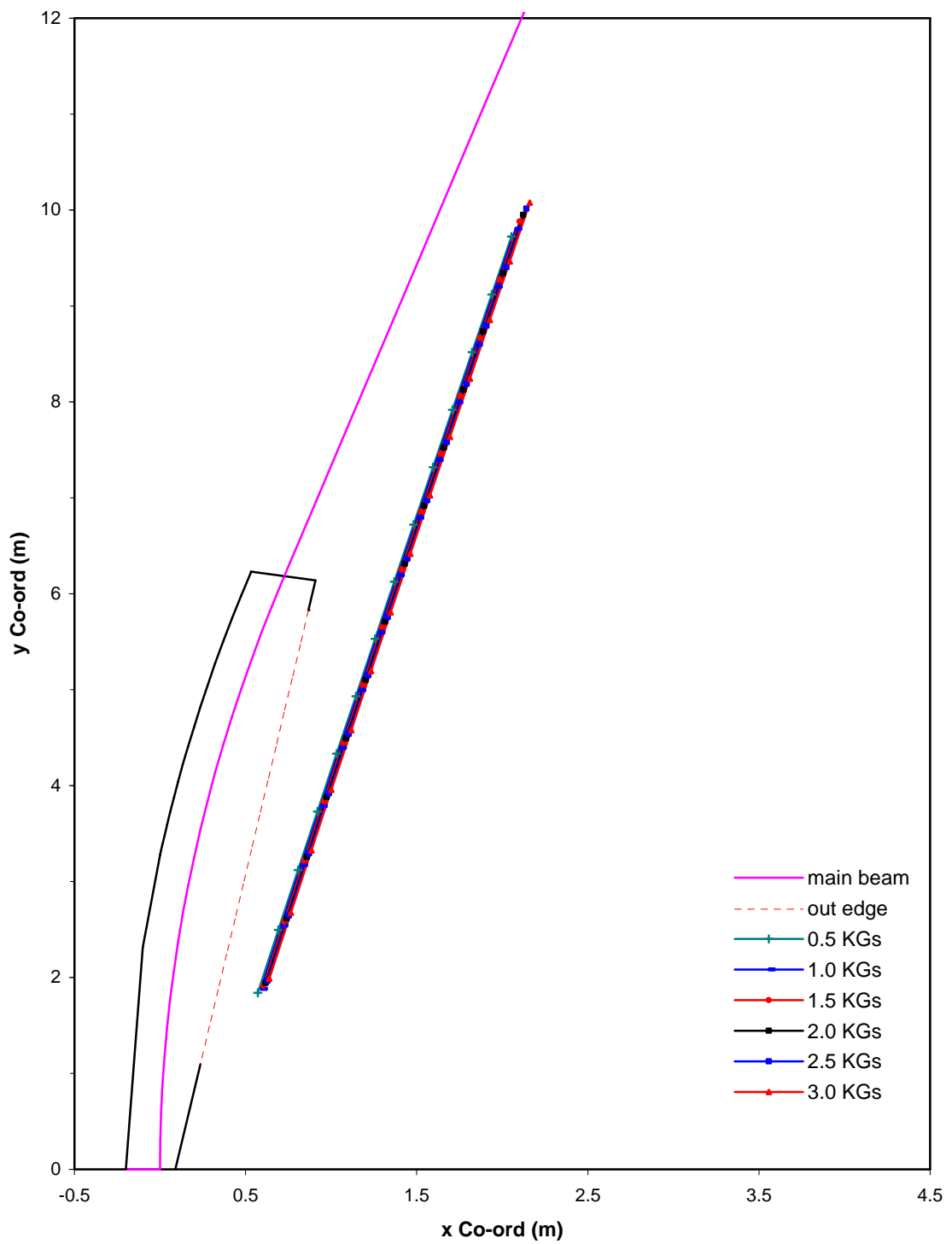


Fig 14 Plan view of magnet geometry and focal plane positions for different quadrupole tip fields.

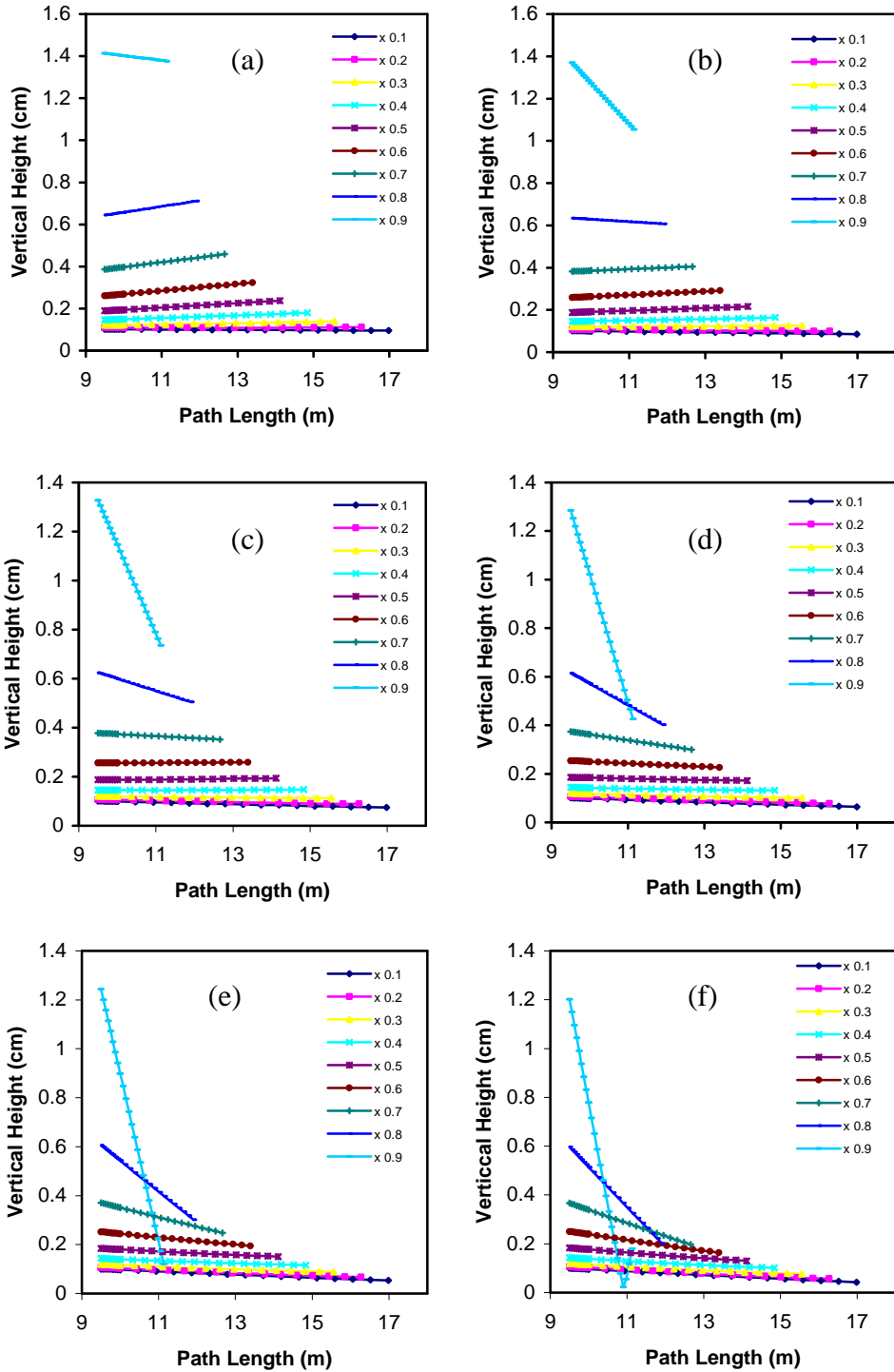


Fig 15 Beam vertical height inside the magnet for different tip fields.  
(a:0.5 KGs, b:1.0 KGs, c:1.5 KGs, d:2.0 KGs, e:2.5 KGs, f:3.0 KGs)

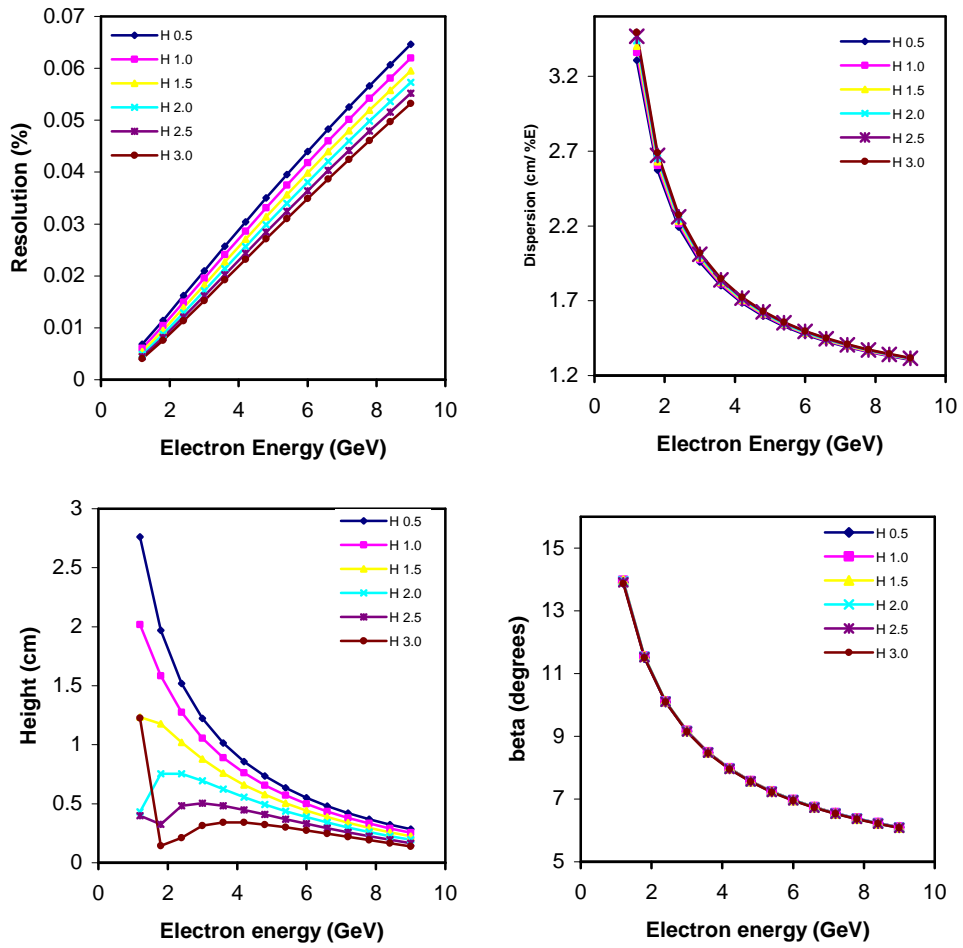


Fig 16 Resolution, dispersion, vertical height, and angle Beta as a function of electron energy for different QD tip fields.

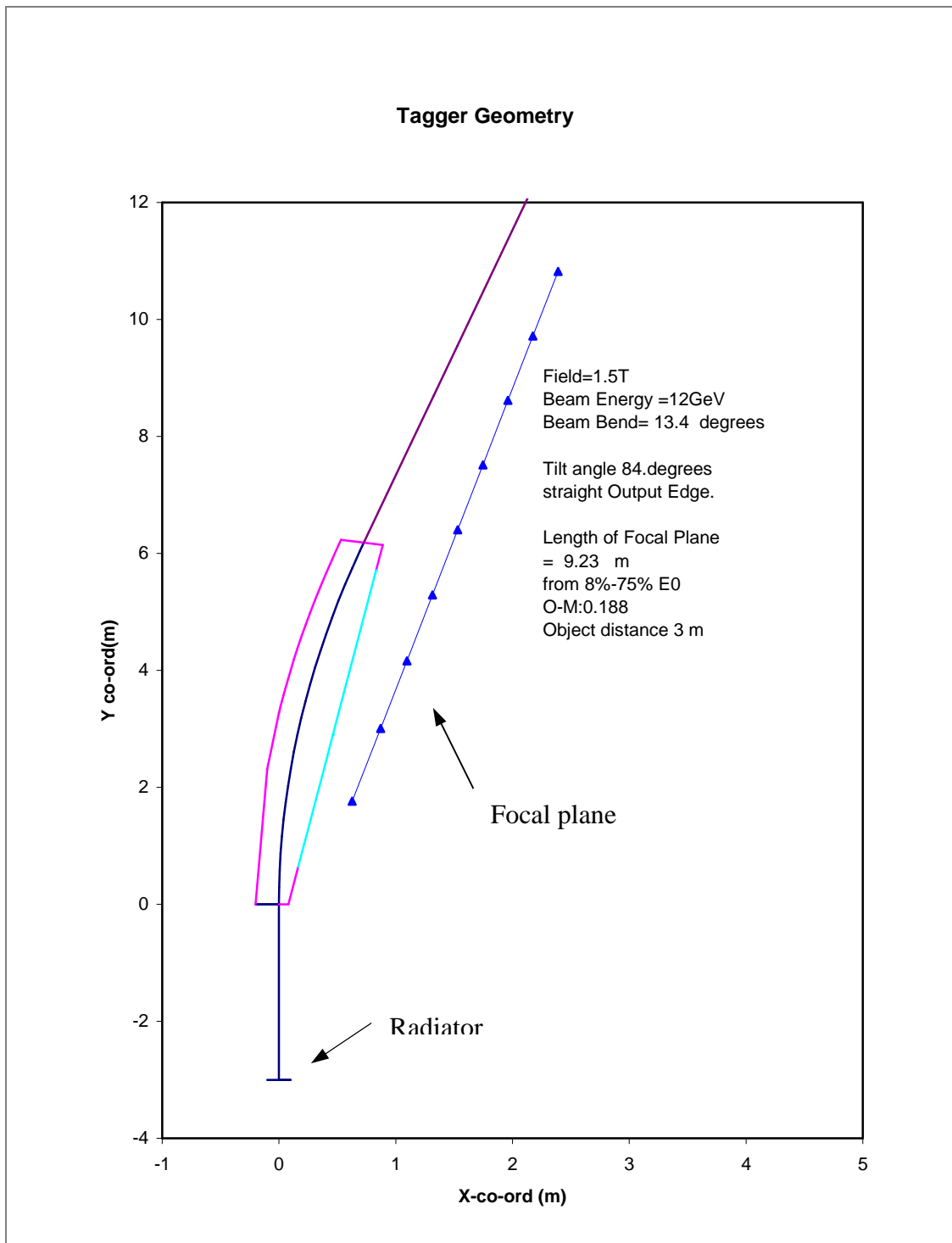


Fig 17.1 Tagger Geometry for a straight output edge with 3m object distance

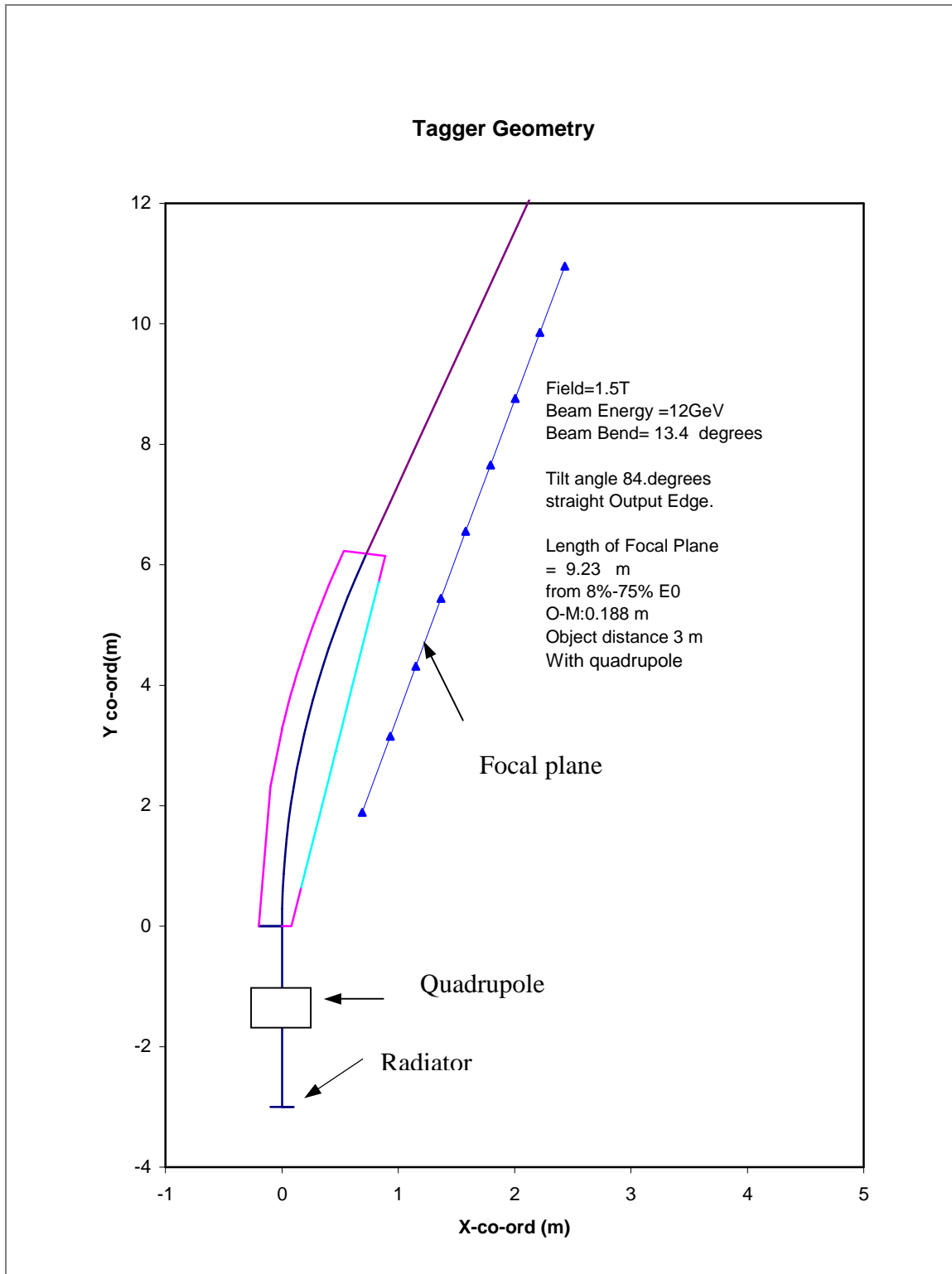


Fig 17.2 Tagger Geometry for the straight output edge with 3m object distance

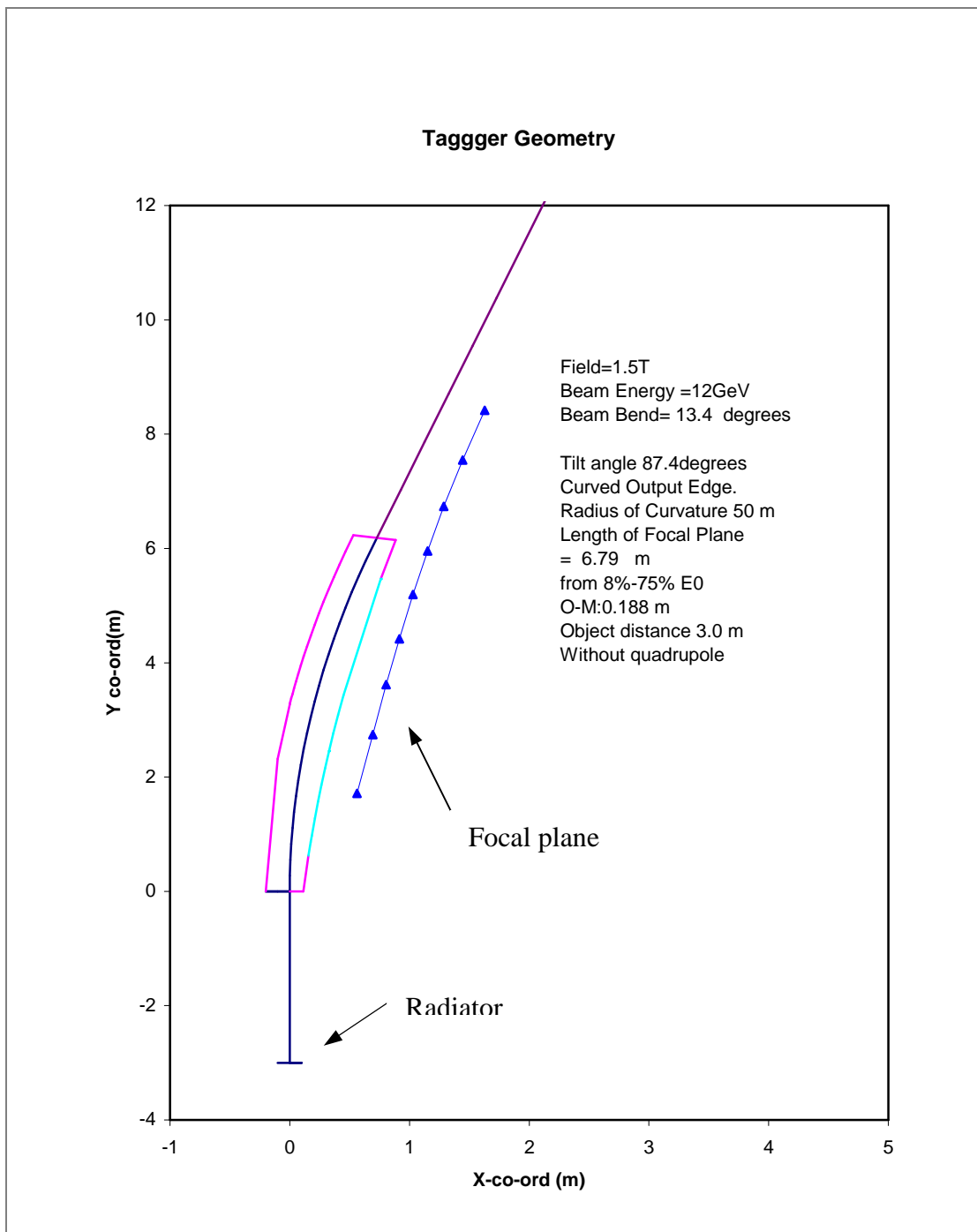


Fig 17.3 Tagger Geometry for the curved output edge with 3m object distance.

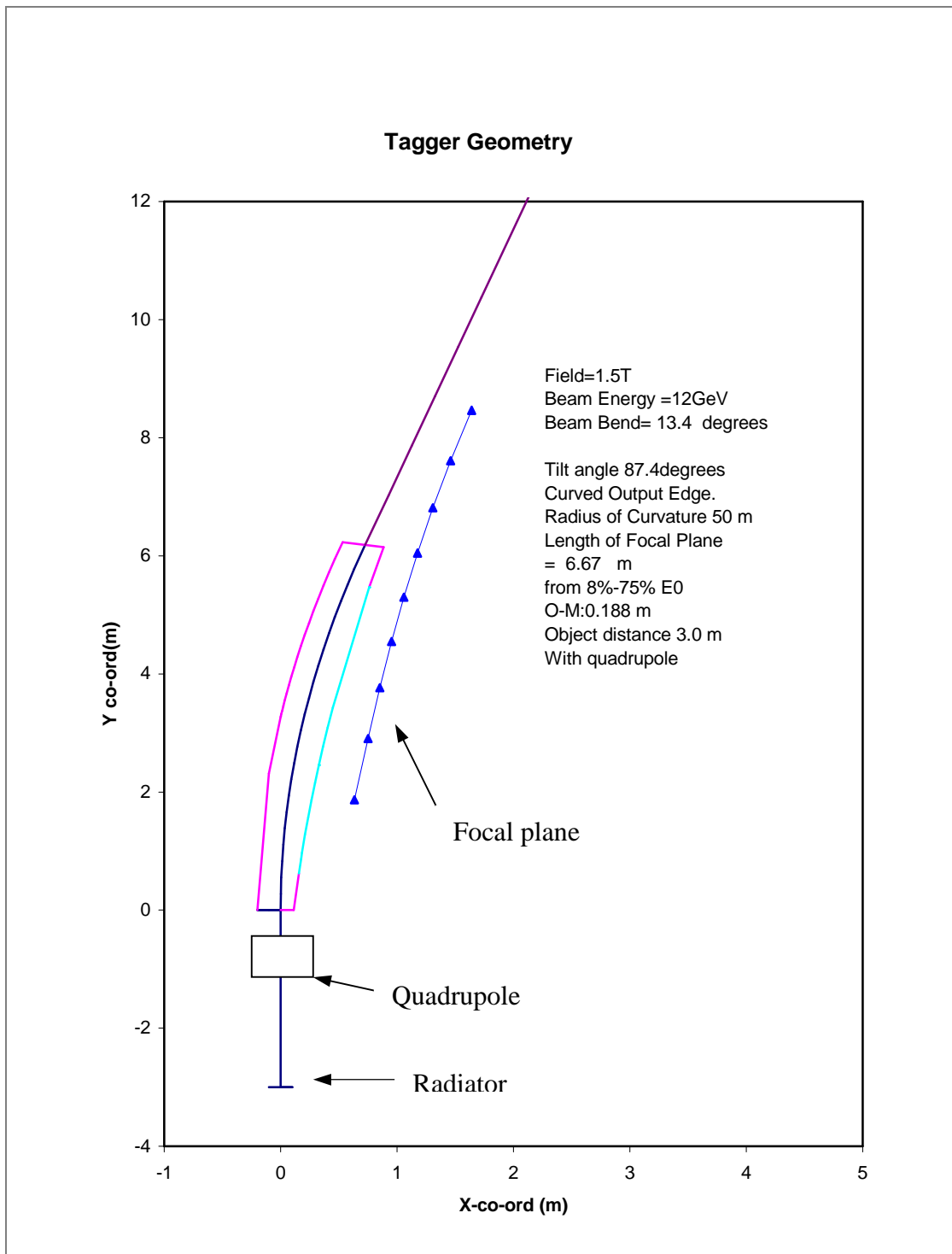


Fig 17.4 Tagger Geometry for the curved output edge with 3m object distance.

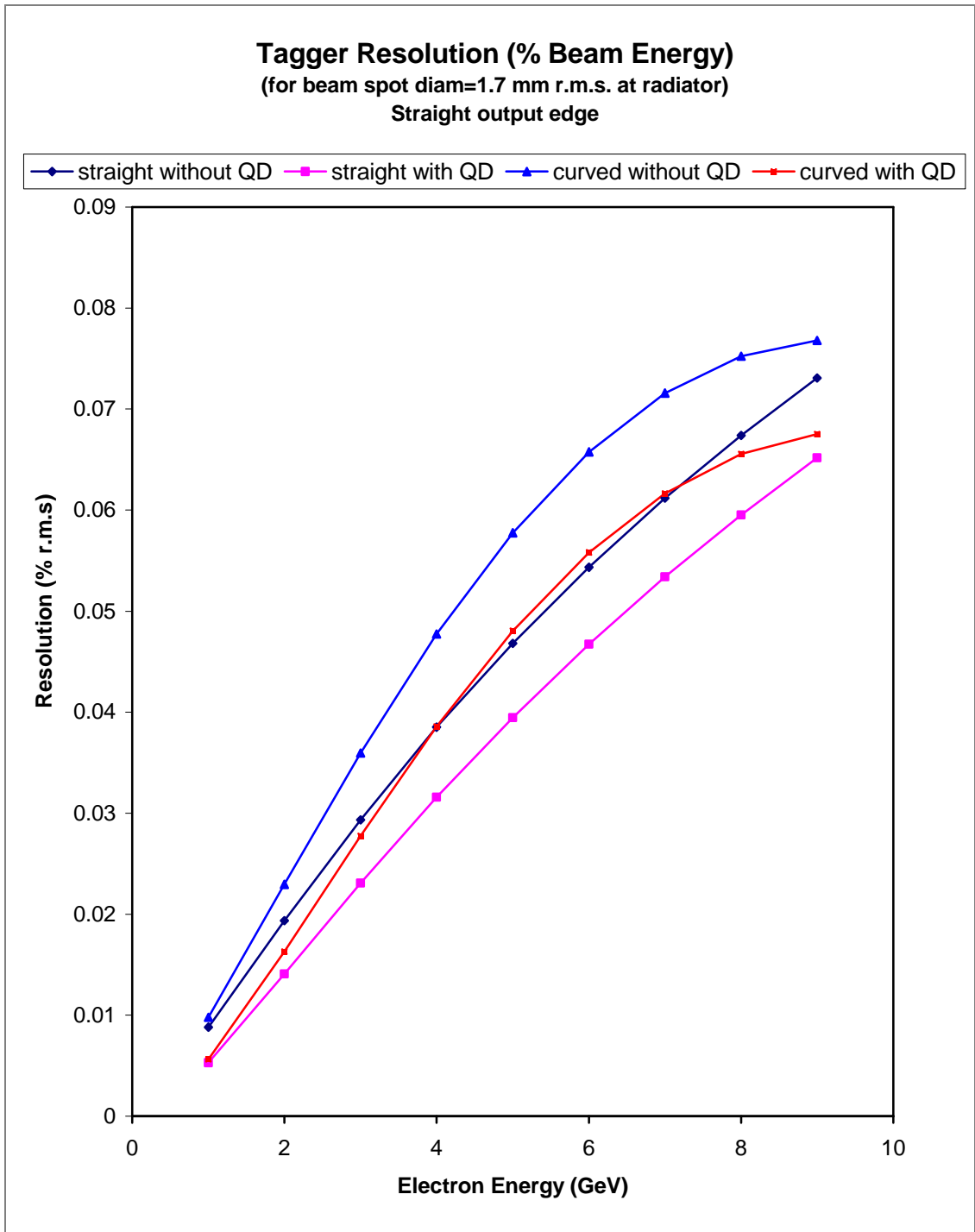


Fig 18.1, Resolution as a function of electron energy for different designs.

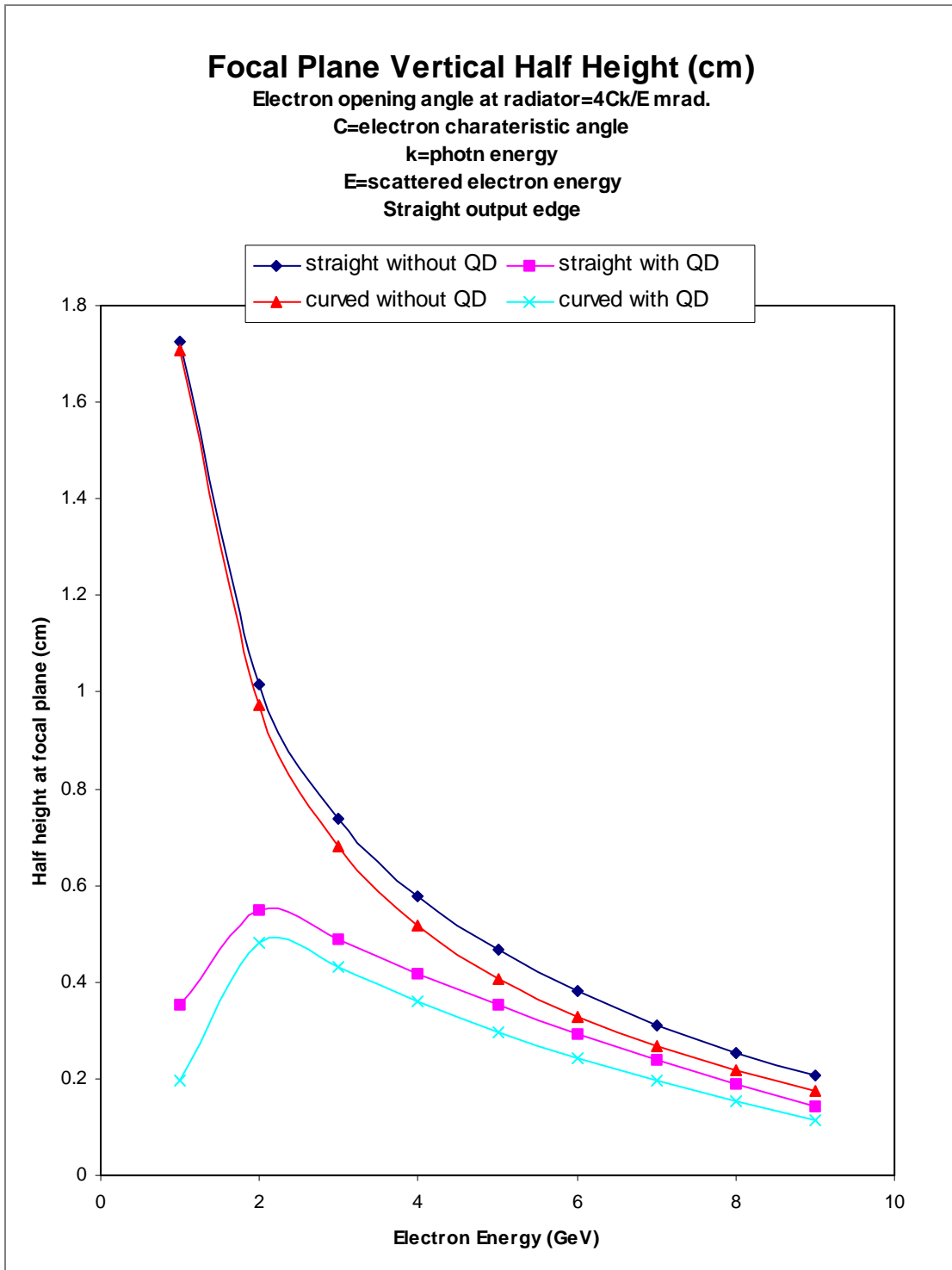


Fig 18.2 . Vertical half height as a function of electron energy for different designs.